



Repetitive Transcranial Magnetic Stimulation-Mediated Neuroprotection in the 5xFAD Mouse Model of Alzheimer's Disease Through GABRG2 and SNAP25 Modulation

Jinyang Wang¹ · Chenming Zhou² · Zhimin Huang³ · Xiaoming Ji^{4,5} · Rui Cui⁵ · Yunxiao Kang^{4,5} · Guoliang Zhang⁵ · Yu Wang⁴ · Tianyun Zhang⁴

Received: 11 March 2024 / Accepted: 6 July 2024

© The Author(s), under exclusive licence to Springer Science+Business Media, LLC, part of Springer Nature 2024

Abstract

Alzheimer's disease (AD) is a leading neurodegenerative disorder with substantial impacts on cognition and behavior. Repetitive transcranial magnetic stimulation (rTMS), a non-invasive neuromodulation technique, has been used to treat various neuropsychiatric disorders, but its efficacy in AD has not been thoroughly investigated. This study examines the neuroprotective effects of rTMS in the 5xFAD mouse model of AD, with a particular focus on its modulation of GABAergic neuronal activity via the GABRG2 and SNAP25 proteins. Transcriptomic sequencing of rTMS-treated 5xFAD mice revealed 32 genes influenced by the treatment, among which GABRG2 was identified as a critical modulatory target. Electrophysiological assessments, including whole-cell patch clamp recordings from frontal cortex neurons, demonstrated significant alterations in inhibitory synaptic currents following rTMS. Subsequent experiments involved sh-GABRG2 transduction combined with rTMS treatment (20Hz, 14 days), examining behavioral responses, GABAergic neuron functionality, cortical GABA expression, cerebrospinal fluid GABA concentrations, β -amyloid accumulation, and pro-inflammatory cytokine levels. The results indicated notable improvements in behavioral performance, enhanced functionality of GABAergic neurons, and reductions in β -amyloid deposition and neuroinflammation after rTMS treatment. Further analysis revealed that SNAP25 overexpression could counteract the negative effects of GABRG2 silencing, highlighting the crucial role of SNAP25 downstream of GABRG2 in mediating rTMS's therapeutic effects in AD. This research highlights rTMS's potential to modulate synaptic and vesicular transport mechanisms, offering a promising avenue for ameliorating symptoms of AD through neuroprotective pathways.

Keywords Alzheimer's disease · Repetitive transcranial magnetic stimulation · GABRG2 · GABA · SNAP25 · Synaptic function · Cerebral cortex · Vesicular transport

Introduction

Alzheimer's disease (AD) is the predominant form of dementia, accounting for 60 to 80% of all cases, and represents a major neurodegenerative disorder particularly prevalent among the elderly [1, 2]. With the aging of the global population, AD increasingly poses significant public health challenges with a rising incidence [3]. The primary pathological features of AD include the accumulation of neurofibrillary tangles formed by hyperphosphorylated tau proteins and extracellular aggregates of amyloid-beta (A β) peptides [4]. Despite extensive research, the pathogenesis of AD remains incompletely understood, and early-stage diagnosis is often complicated by the absence of distinct clinical symptoms [5]. Current pharmacological treatments

✉ Tianyun Zhang
zhangtianyun@hebmu.edu.cn

¹ Department of Neurology, The Third Hospital of Hebei Medical University, Shijiazhuang 050051, China

² Core Facilities and Centers, Hebei Medical University, Shijiazhuang 050017, China

³ Department of Stomatology, People's Hospital, Shizhu Tujia Autonomous County, Chongqing 409100, China

⁴ Laboratory of Neurobiology, Hebei Medical University, Zhongshan Donglu No.361, Shijiazhuang Hebei Province 050017, China

⁵ Neuroscience Research Center, Hebei Medical University, Shijiazhuang 050017, China

primarily offer symptomatic relief, as definitive therapeutic strategies are yet to be established [6].

In recent years, non-invasive neuromodulation techniques, particularly repetitive transcranial magnetic stimulation (rTMS), have received considerable attention in recent research [7–10]. rTMS, which modulates neuronal activity through magnetic fields, is celebrated for its non-invasiveness, safety, and repeatability. It has been successfully employed in the treatment of various neuropsychiatric conditions, including depression and anxiety [11]. Promisingly, rTMS has emerged as a potential therapeutic option for AD, proposing benefits in modulating neural networks and enhancing cognitive functions. The technique also enables real-time monitoring of cognitive effects and brain dynamics via electroencephalography [12]. Clinical trials involving early to middle-stage AD patients have shown that high-frequency rTMS significantly improves cognitive functions and daily living capabilities, more so than its low-frequency counterpart [13, 14]. Furthermore, evidence suggests that rTMS may enhance A β clearance by modulating the brain's drainage system, as observed in the 5xFAD mouse model [15]. Despite these advances, the research on rTMS as a treatment for AD is still in its early stages, and both its mechanisms and therapeutic efficacy require further rigorous investigation [16].

Interestingly, GABRG2, a key gamma-aminobutyric acid (GABA) receptor subunit, is closely associated with neural inhibition and synaptic plasticity [17]. GABA, the primary inhibitory neurotransmitter in the central nervous system, is pivotal in modulating neuronal excitability [18–20]. Extensive research underscores the critical role of GABAergic neurons in the pathogenesis of AD, linking their functionality to neuronal demise, synaptic impairment, and memory deterioration [21]. Therefore, an in-depth understanding of the contributions of GABRG2 and GABAergic neurons to the pathophysiology of AD is imperative.

Synaptosomal-associated protein 25 (SNAP25), a crucial vesicle fusion protein involved in neurotransmitter release, has been shown to regulate synaptic function and maintain the balance of neurotransmitter release and neuronal excitability [22]. Moreover, SNAP25 is potentially associated with A β deposition, neuroinflammation, and other neurodegenerative changes in AD [23]. Thus, exploring the role of SNAP25 in AD and its interrelationships with GABRG2 and GABAergic neurons is critical for elucidating the potential mechanisms of rTMS therapy in treating AD.

To address this research gap, our study hypothesized that rTMS might influence the behavioral characteristics, neuronal functionality, GABA expression, A β deposition, and neuroinflammation. This study aimed to bridge the existing gap by elucidating the regulatory effects of rTMS through GABRG2 on GABAergic neuron function and its therapeutic effects via the activity of SNAP25, thereby providing

insights into the potential therapeutic mechanisms of rTMS in treating this neurodegenerative disorder.

Materials and Methods

Experimental Animals

C57Bl/6 mice (4-month-old, 20–25 g) were used for AD modeling. These mice were purchased as 5xFAD transgenic specimens from Vital River Laboratory Animal Technology Co., Ltd. (Beijing, China), and acquired from The Jackson Laboratory (006554, USA). These transgenic 5xFAD mice, known for expressing five mutations in the familial AD amyloid precursor protein (APP) and presenilin 1 (PSEN1) genes under the neuron-specific Thy1 promoter, were acquired from Vital River Laboratory Animal Technology Co., Ltd. (Beijing, China), and The Jackson Laboratory (006554, USA). These genetic alterations lead to accelerated cerebral amyloid deposition, a hallmark of AD pathology [24]. Experimental animals were cared for in accordance with the principles of the Guide for the Care and Use of Laboratory Animals under a protocol approved by the Animal Ethics Committee of Hebei Medical University.

The choice of this age range is informed by the typical onset of A β deposition lesions within 2–4 months of age in this strain [25]. Given that 5xFAD mice exhibit sex-specific variations in amyloid pathology [24], the study was restricted to male mice to ensure consistency in the experimental outcomes. The 5xFAD line was developed by cross-breeding with the C57Bl/6 strain. All selected mice were housed under controlled conditions, with the room temperature maintained at 23 ± 2 °C and relative humidity kept at $50 \pm 10\%$. They were provided ad libitum access to water and standard feed, ensuring their well-being and consistency in dietary intake [25]. This controlled environment was established to mitigate external variables that might influence the progression of AD-like symptoms in the transgenic models.

Construction of Silencing Lentivirus

Lentiviral packaging services were provided by Sangon Biotech (Shanghai, China). The pHAGE-puro vector plasmids along with helper plasmids pSPAX2 and pMD2.G and the pSuper-retro-puro vector plasmids along with helper plasmids gag/pol and VSVG were co-transfected into 293T cells (CRL-3216, ATCC, USA). The supernatant was collected 48 h later, filtered through a 0.45 μ m filter, and the virus was subsequently harvested. The supernatant was collected again 72 h later and centrifuged to concentrate. The viruses from both collections were mixed, and their titers were determined. The sequences for silencing and overexpressing lentiviruses, listed in Table S1, were validated for silencing

efficacy in the HT22 hippocampal neuronal cell line (CRL-2260, ATCC, USA; Fig. S1). The silencing sequence (sh-GABRG2-1) with the highest efficiency was selected for further experiments.

rTMS Treatment Protocol

The rTMS was administered using a magnetic stimulator (CCY-II, Wuhan Yiruide Medical Equipment, Wuhan, China). During the treatment sessions, 5xFAD mice were confined within a custom-made fabric sleeve, which restricted their movement except for their heads. The mice exhibited normal respiration and showed no signs of distress during the rTMS stimulation. A circular coil with a diameter of 6.5 cm was positioned to center over the mouse's head. The rTMS was delivered daily at a consistent time for 14 days, consisting of 20 bursts at 20 Hz, with each burst lasting 2 s and an intensity set at 1.38 T, interspersed with 1-s intervals [15]. After 14 days of treatment, a 7-day recovery period was allowed for the mice [26].

Animal Grouping

To assess the impact of GABRG2 on mouse behaviors, C57BL/6 mice were randomly divided into three groups of six each: (1) Normal group: untreated, (2) sh-NC group: subjected to transduction with an empty vector lentivirus, (3) sh-GABRG2 group: subjected to transduction with a GABRG2 silencing lentivirus. All lentiviral injections were administered intracerebrally at 1×10^7 TU.

To determine the potential of rTMS to ameliorate AD-like behaviors in 5xFAD mice via GABRG2 modulation, both C57BL/6 and 5xFAD mice were divided into the following four groups of six each: (1) WT group: untreated C57BL/6 mice, (2) AD group: untreated 5xFAD mice, (3) AD + rTMS group: 5xFAD mice treated with the aforementioned rTMS protocol, (4) AD + sh-GABRG2 + rTMS group: 5xFAD mice subjected to GABRG2 silencing lentiviral transfection, followed by a 7-day recovery period and subsequent rTMS treatment. Lentiviral administrations were carried out intracerebrally with a dosage of 1×10^7 TU.

To examine the role of the downstream key gene SNAP25, an overexpression lentiviral vector group (viral titer of 10^8 TU) was used, designed, and synthesized by Suzhou Genecreate Biological Engineering Co., Ltd. (Suzhou, China). The 5xFAD mice were divided into two groups of six each: (1) AD + sh-GABRG2-rTMS group: 5xFAD mice subjected to GABRG2 silencing lentiviral transduction followed by the rTMS treatment and (2) AD + sh-GABRG2 + OE-NC + rTMS group and 3) AD + sh-GABRG2 + OE-SNAP25 + rTMS group: 5xFAD mice subjected to GABRG2 silencing and SNAP25 overexpression lentiviral transductions followed by rTMS treatment.

Lentiviral administrations were performed intracerebrally at a dose of 1×10^7 TU [26].

Open Field Test

The experimental setup for the open field test comprised a square arena, segmented into four quadrants, each measuring 50 cm \times 50 cm \times 40 cm. Boundaries were marked on the floor. Mice were placed in the arena and given a 30-s period for acclimatization. Subsequently, each mouse was then observed for 10 min, and their activities were recorded by a video camera positioned 120 cm from the test area. The time spent in the central area (where all four limbs remained within the central square) and the distance traveled within this area were measured under normal lighting conditions (800 lx) [27].

Three-Chamber Social Interaction Test

This test was conducted in a three-chambered box (60 \times 44 \times 40 cm³), with openings between chambers that could be covered by glass panels during certain phases. Initially, mice were placed in the empty apparatus to freely explore all chambers for 10 min. Subsequently, an unfamiliar mouse from a different litter was confined in a metal cage within the left chamber. The test mice were then permitted to explore all chambers, and the duration of interaction with the first unfamiliar mouse and the time spent in the empty chamber were recorded over 10 min. For the social novelty phase, a second unfamiliar mouse was introduced into the previously empty chamber after the openings had been sealed. Upon removal of the barriers, the test mice were allowed an additional 10-min exploration period, during which the time spent interacting with the second unfamiliar mouse was documented. This experiment aimed to assess the preference of mice for novel social interactions [28].

Y-Maze Alternation Test

The Y-maze used for this test included a central starting area and three branching arms, each sized at 45 cm \times 10 cm \times 15 cm, with reward food placed at the end of each branch. Mice were initially placed in the starting area to acclimate to the maze environment. Their behavior, including exploration, duration of stay, and branch entries, was recorded using a camera. Subsequently, the mice were trained to familiarize themselves with the layout and locations of the food. During the testing phase, the food's location was altered to assess the spatial learning and memory capabilities of mice. Data concerning exploration time, the number of entries into different branches, and the accuracy of locating the reward were analyzed [29].

Morris Water Maze Test

A circular pool, measuring 120 cm in diameter and 50 cm in height, was filled with colorless, transparent water, and maintained at a temperature close to that of the mouse's body. A circular escape platform, 15 cm in diameter, was submerged 2 cm below the water's surface at a fixed location within the pool and coated with an opaque color to render it less visible underwater. Mice were first allowed to adapt to the experimental environment, including the testing room and the pool, to reduce stress responses. They were then placed at various starting points around the pool, and their behavior was recorded. Training sessions ensued, with visual cues provided to denote the platform's location. Following training, the cues were removed, and the mice's ability to locate the escape platform without cues was evaluated [30].

Transcriptome Sequencing

Tissue samples (20–50 mg) from the frontal cortex of mice in the sh-GABRG2 group, sh-NC group, AD group, and AD + rTMS group were sectioned on dry ice. Total RNA was extracted using TRIzol (ThermoFisher, USA). The purity and concentration of the extracted RNA were assessed using a Nanodrop 2000 spectrophotometer (ThermoFisher, USA). According to the instructions of the PrimeScript RT reagent Kit (RR047A, Takara, Japan), the RNA was reverse-transcribed into cDNA for transcriptomic sequencing. Differential gene analysis was conducted using the R package "limma," with $\log_2(\text{FoldChange}) > 2$ and significance $p < 0.05$ as the criteria for selection of differentially expressed genes (DEGs) [31].

Bioinformatics Screening of DEGs for rTMS in AD

Candidate targets for rTMS in AD were screened through the ProteomeXchange proteomics public database (<http://www.proteomexchange.org>), specifically retrieving the PXD025261 dataset under the entry "Alzheimer's Disease." This search yielded proteomic results of frontal cortex samples from AD patients. Intersection analysis of these differentially expressed proteins (DEPs) with DEGs from transcriptomic sequencing was performed to identify potential targets for rTMS treatment in AD. Venn analysis was conducted online (<https://www.xiantao.love/>) to visualize the intersecting results [32, 33].

Protein-Protein Interaction (PPI) Network Analysis

Protein-protein interaction analysis of the candidate targets for rTMS treatment in AD was performed using the STRING database (<https://string-db.org>). The species was specified as "Homo sapiens" and the confidence level was set to the

highest (0.900). Disconnected nodes were excluded, and default settings were utilized. The PPI network relevant to the disease was then imported into Cytoscape 3.7.2, where key targets were identified employing the MCC algorithm within the cytoHubba plugin [34, 35].

Functional Enrichment Analysis of Candidate Targets

Functional enrichment analysis of gene sets was carried out using online analysis software (<http://vip.sangerbox.com/login.html>), the DAVID database (<https://david.ncifcrf.gov/home.jsp>), and the R package org.Hs.eg.db (version 3.1.0) for GO annotations. Genes were mapped to the background set, and enrichment analysis was performed using the R package clusterProfiler (version 3.14.3). The criteria for the analysis were established with a minimum gene set of 5 and a maximum of 5000, with p values < 0.05 and FDR < 0.1 [32].

Collection of Cerebrospinal Fluid (CSF) Samples

Mice were anesthetized with isoflurane to achieve muscle relaxation and then positioned laterally on a surgical table. The spine was exposed using a surgical scalpel from the dorsal side. A lumbar puncture was performed with a microsyringe, penetrating the CSF chamber and gently extracting 5–10 μL of CSF. Following extraction, the samples were immediately transferred to collection tubes and stored at -80°C for subsequent analysis via ELISA [36].

ELISA

The GABA ELISA kit (YS02798B, Shanghai Yaji Biological Technology, Shanghai, China) was utilized for the assay. The wells of the ELISA plate were blocked with 5% fetal bovine serum (F8318, Merck, Wuhan, China) to prevent nonspecific binding. In the wells, diluted samples, enzyme-labeled antibodies, and substrate solution were added, and the reaction was terminated by the addition of 50 μL of stop solution within 20 min. The absorbance was measured at 450 nm using a spectrophotometer (Bio-Rad, USA), and a standard curve was constructed for data analysis [37].

Preparation of Brain Slices

Following anesthesia with isoflurane, brain tissues were rapidly extracted and immersed in chilled artificial cerebrospinal fluid (ACSF) containing 250 mM sucrose, 26 mM NaHCO_3 , 10 mM glucose, 10 mM MgSO_4 , 2 mM KCl, 1.3 mM NaH_2PO_4 , and 0.2 mM CaCl_2 . Brain slices,

including the frontal cortex, 400 μm thick, were prepared using a vibratome (VT-1200s, Leica, Germany) in chilled modified ACSF. The slices were then transferred to a holding chamber containing standard ACSF (126 mM NaCl, 26 mM NaHCO_3 , 10 mM glucose, 3 mM KCl, 2 mM CaCl_2 , 1.25 mM NaH_2PO_4 , and 1 mM MgSO_4), where they were allowed to recover at 34 °C for 30 min and at room temperature (25 ± 1 °C) for 1 h before recordings commenced. Throughout the preparation process, all solutions were saturated with 95% O_2 /5% CO_2 (volume ratio) [38].

Electrophysiological Recordings

Prepared brain slices were positioned in a perfusion chamber and perfused with ACSF at a flow rate of 3 mL/min at 30–32 °C. Neuronal activity within the slices was recorded under an infrared differential interference contrast microscope (ECLIPSE FN1, Nikon) using whole-cell patch-clamp techniques. During recordings in current clamp mode, continuous hyperpolarizing and depolarizing current pulses (500 ms) at 0.2 Hz were applied to characterize the intrinsic membrane properties and firing characteristics of endogenous neurons. For recordings of inhibitory postsynaptic currents (sIPSCs), the holding potential of the patch electrode was maintained at 0 mV. The intracellular solution in the patch electrode (input resistance: 3 M Ω) consisted of 110 mM Cs_2SO_4 , 0.5 mM CaCl_2 , 2 mM MgCl_2 , 5 mM EGTA, 5 mM HEPES, 5 mM TEA, 5 mM ATP-Mg at pH 7.35, and 285 mOsm. For recording miniature inhibitory postsynaptic currents (mIPSCs), the intracellular solution included 115 mM cesium methanesulfonate, 20 mM CsCl, 10 mM HEPES, 2.5 mM MgCl_2 , 10 mM sodium phosphocreatine, 5 mM QX-314, 4 mM $\text{Na}_2\text{-ATP}$, 0.4 mM $\text{Na}_3\text{-GTP}$, and 0.6 mM EGTA (pH, 7.3; 285 mOsm).

Synaptic responses were induced by positioning stimulating electrodes approximately 0.2 mm from the thalamic fiber pathways to the frontal cortical neurons. Electrical stimulation was delivered at 30-s intervals at holding potentials of +40 mV for NMDAR-mediated responses, –70 mV for AMPAR-mediated responses, or 0 mV for GABAA receptor-mediated responses. NMDAR-mediated responses were quantified based on the amplitude of currents 50 ms post-stimulation. For the recording of evoked IPSCs, stimulation electrodes were placed no more than 0.05 mm away from the cell body; to isolate bilateral inhibitory IPSCs, 20 μM CNQX and 100 μM D,L-APV were added to the ACSF. Data were recorded with a multiClamp 700B amplifier, digitized at 5 kHz, and filtered at 1 kHz. Data collection was conducted when series resistance fluctuated within 20% of the initial value, and results were analyzed using pClamp 10.2 software [39].

Spike Probability Measurement

Prepared slices from the frontal cortical tissue were maintained in ACSF for 60 min before transfer to a recording chamber. In oxygenated ACSF, isolated units were stimulated at 0.1 Hz through lateral vein pathway fibers to elicit neuronal synaptic responses. Evoked EPSPs were recorded using glass pipette electrodes filled with 120 mM potassium gluconate, 10 mM KCl, 1 mM MgCl_2 , 0.5 mM EGTA, and 40 mM HEPES. The ratio of successful spike-inducing stimuli to the total number of stimuli was calculated as the spike probability. Data were collected using a multiClamp 700B and Clampex 10 software, digitized with a Digidata 1322A, low-pass filtered at 4 kHz, and analyzed offline at a sampling rate of 10 kHz using pClamp 10.2 software [40].

Preparation of Brain Cryosections

Mouse brain tissues were extracted and fixed overnight at 4 °C using 4% paraformaldehyde, followed by immersion in 30% sucrose for 48 h for cryoprotection. The tissues were then positioned on a cryostat and sectioned into 30- μm coronal frontal cortex slices. These sections were subsequently immersed in PBS and rinsed three times. After preparation, the sections were utilized for subsequent staining studies [41].

Immunohistochemistry Staining

Following the preparation of cryosections, the sections were incubated for 1 h in a blocking solution (0.3% Triton-X, 2% normal serum in 0.1M PBS). The sections were then incubated overnight at 4 °C with primary antibodies: mouse anti-GABRG2 (ab307231, 1:500, Abcam, USA), rabbit anti-SNAP25 (ab109105, 1:250, Abcam), rabbit anti-synaptotagmin-1 (SYT1) (ab302627, 1:500, Abcam), and rabbit anti-vesicle-associated membrane protein 2 (VAMP2) (ab215721, 1:2000, Abcam) in blocking solution. Afterward, the sections were washed three times with PBS, followed by a 30-min incubation with 100 μL of enzyme-labeled goat anti-mouse/rabbit IgG polymer (pv6000, Zhongshan Goldenbridge, China). The sections were then developed using a DAB staining kit (ZLI-9018, Zhongshan Goldenbridge, China) and observed under a microscope. Images were captured for one section per animal, with six animals per group. The area of positive staining was quantified using ImageJ 1.48u software (V1.48, National Institutes of Health, USA) [41].

Immunofluorescent Staining

Prepared cryosections were incubated for 1 h in a blocking solution containing 0.3% Triton-X and 2% normal serum in

0.1M PBS. Primary antibodies were then applied: mouse anti-GABA (ab86186, 1:200, Abcam, USA) or mouse anti-beta Amyloid (A β) (ab224026, 1:200, Abcam, USA), and the sections were incubated overnight at 4 °C. After three washes with PBS, the sections were incubated for 3 h with goat anti-mouse IgG(H + L) secondary antibody conjugated with fluorescence (A0473, Beyotime, China), followed by three more washes with PBS. Sections were then mounted using an anti-fade mounting medium with DAPI (P0131, Beyotime, China), and images were acquired using a fluorescence microscope. For each of the six animals per group, one section was stained, and an image was captured from one selected field of view. Positive area percentages were calculated using ImageJ 1.48u software (V1.48, National Institutes of Health) [42].

Western Blot Analysis

Mouse frontal cortex tissues were homogenized in RIPA lysis buffer (P0013B, Beyotime Biotechnology, China) supplemented with protease inhibitors (P1005, Beyotime, China). After thorough homogenization, the mixture was left to stand at 4 °C for 1 h before being centrifuged at 12,000 rpm for 15 min. The supernatant was collected and stored at -80 °C. Protein concentrations were quantified using the BCA Protein Assay Kit (A53226, Thermo Fisher Scientific, Rockford, IL, USA). Proteins were then transferred from the gel to a PVDF membrane (IPVH85R, Millipore, Darmstadt, Germany) using the wet transfer method. After blocking with 5% BSA at room temperature for 1 h, the membrane was incubated with primary antibodies against GABRG2 (ab288564, 1:1000, Abcam, USA), SNAP25 (ab109105, 1:1000, Abcam, USA), SYT1 (ab302627, 1:1000, Abcam, USA), TNF- α (ab183218, 1:1000, Abcam, USA), IL-1 β (ab254360, 1:1000, Abcam, USA), IL-6 (ab233706, 1:1000, Abcam, USA), and β -actin (3700, 1:1000, Cell Signaling Technology, USA). Following incubation, the membrane was washed and then incubated with HRP-conjugated secondary antibody goat anti-rabbit IgG (ab6721, 1:5000, Abcam) for 2 h. The membrane was washed thrice with TBST for 5 min each and visualized using a chemiluminescence detector. Protein levels were quantified using ImageJ 1.48u software, as normalized to the internal control β -actin [43].

RT-qPCR

Total RNA was extracted from tissues using TRIzol (15596026, ThermoFisher, USA), and its purity and concentration were assessed using a Nanodrop 2000 spectrophotometer (ThermoFisher, USA). Following the manufacturer's instructions of the PrimeScript RT reagent Kit (RR047A, Takara, Japan), RNA was reverse-transcribed

into cDNA. Subsequently, RT-qPCR was performed using the Fast SYBR Green PCR Kit (11736059, Thermo Fisher Scientific, Shanghai, China). Each reaction was set up in triplicate, with GAPDH serving as the internal reference. Relative gene expression was calculated using the $2^{-\Delta\Delta C_t}$ method [44], with primer sequences detailed in Table S2.

Statistical Analysis

All data were processed using GraphPad Prism 8.0. Quantitative data were presented as mean \pm standard deviation (mean \pm SD). An unpaired *t* test was utilized to compare two groups, while one-way ANOVA was employed to compare multiple groups. Homogeneity of variances was assessed using Levene's test. Dunnett's *t* and LSD-*t* tests were applied for pairwise comparisons when variances were equal; otherwise, Dunnett's *T3* test was used. Pearson analysis was conducted to evaluate correlations between genes and between gene expressions and immune cell content [45]. A *p*-value < 0.05 was considered statistically significant.

Results

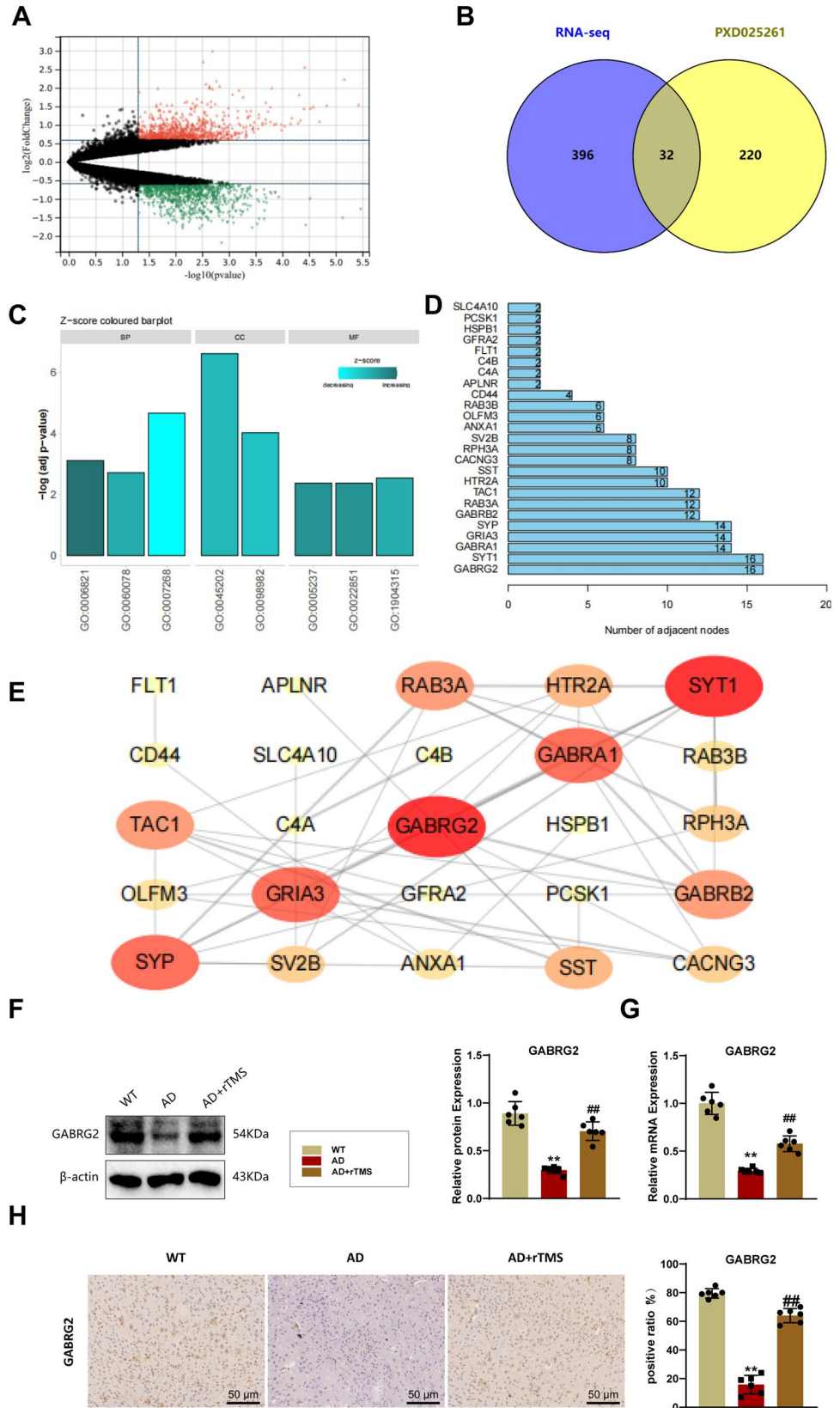
Identification and Functional Analysis of Key Genes in rTMS Treatment of AD

To elucidate the neurophysiological mechanisms underlying the function of rTMS in treating AD, transcriptomic sequencing was performed on frontal cortex tissues of 5xFAD mice in the presence or absence of rTMS treatment. DEG analysis identified 428 genes, with 200 upregulated and 228 downregulated, using a threshold of $|\log_2(\text{FoldChange})| > 2$ and *p* < 0.05 (Fig. 1A, Table S3). Subsequently, DEPs expressed in the frontal cortex of AD patients were retrieved from the ProteomeXchange proteomics public database to pinpoint key genes, resulting in 252 DEPs (Table S4). These proteins were intersected with the 428 DEGs from the transcriptomic data, yielding 32 candidate genes (Fig. 1B).

Bioinformatics analysis was furthered with a GO functional analysis of the 32 candidate genes based on a *p*-value adjustment threshold of < 0.05 (Fig. 1C). The top 20 entries in the GO functional analysis included cellular components such as synaptic vesicle membrane and neuron projection, biological processes like chemical synaptic transmission and chloride transport, and molecular functions including inhibitory extracellular ligand-gated ion channel activity (Fig. S2A-D).

These 32 candidate proteins were imported into the STRING database to analyze their interactions, visualized in a node graph based on Degree value, and a PPI network was constructed using Cytoscape software (Fig. 1D-E).

Fig. 1 Identification of key genes in AD treated with rTMS using transcriptomic and proteomic databases. **A** DEG expression analysis of transcriptomic sequencing data from the frontal cortex samples of 5xFAD mice receiving or not receiving rTMS treatment using a volcano plot. **B** Intersection analysis of DEPs and genes identified by the transcriptomic sequencing using the Proteome X Change database PXD025261. **C** Histogram showing the Gene Ontology (GO) enrichment results for the 32 DEGs. **D** Interaction network analysis of the 32 candidate target proteins, showing the degree values. **E** PPI network was constructed using the STRING database and Cytoscape software for the 32 candidate genes. Larger circles with deeper background colors represent higher degree values. **F** Western blot analysis and statistical column chart of the expression level of GABRG2 in the frontal cortex of mice in different groups. **G** RT-qPCR analysis of the mRNA level of GABRG2 in the frontal cortex of mice in different groups. **H** Immunohistochemical staining to examine the expression level of GABRG2 in the frontal cortex tissue of mice in different groups. * $p < 0.05$, ** $p < 0.01$ compared to the WT group. # $p < 0.05$, ## $p < 0.01$ compared to the AD group. Data were compared using an unpaired t test. $n = 6$. Scale bar = 50 μm



GABRG2 was identified with the highest node degree among the interaction nodes.

Evidence exists indicating that GABRG2 encodes the $\gamma 2$ subunit of GABA_A receptors (GABA_{AR}s), influencing their assembly, chloride channel permeability, and postsynaptic localization and clustering [46]. Mutations in GABRG2 can affect GABA_{AR} gating, membrane trafficking, and synaptic clustering, which are integral to the progressive synaptic dysfunction and loss typical in AD pathology [47].

To validate the bioinformatics findings, the 5xFAD transgenic mice were used as AD models, and their response to rTMS treatment was observed. Western blot analysis revealed that, compared to controls, GABRG2 expression was significantly downregulated in the AD group ($p < 0.01$) and was notably restored in the AD + rTMS treated group ($p < 0.01$) (Fig. 1F). RT-qPCR analysis of GABRG2 mRNA levels in the frontal cortex samples from various groups corroborated these findings (Fig. 1G). Furthermore, immunohistochemical staining showed a significant reduction in the positive staining area of GABRG2 in the AD group compared to the WT group, which significantly increased following rTMS treatment (Fig. 1H).

Thus, bioinformatics and molecular biology analyses of mouse brain cortical tissues unveiled that GABRG2 might be a potential target for rTMS treatment in AD.

Behavioral Impact of GABRG2 Knockdown in Mice with AD-Like Phenotypes

The study moved to examine the impact of GABRG2 expression changes. Therefore, the GABRG2-silenced mouse model (sh-GABRG2) was developed using lentiviral transfection, alongside a control group receiving an empty vector (sh-NC). Following a 7-day recovery period, behavioral assessments were conducted (Fig. 2A).

Considering that social behavior and cognitive deficits are hallmark features of various neuropsychiatric disorders, including AD, the three-chamber social interaction test was employed to evaluate the effects of GABRG2 knockdown on social behavior and social novelty (Fig. 2B). The movement trajectories of the test mice are shown in (Fig. 2C), revealing a significant reduction in the time spent with unfamiliar mice compared to the control group ($p < 0.01$) (Fig. 2D).

Prior research suggests that mutations in GABRG2 can increase anxiety in mice [48]. Given that increased anxiety and reduced exploratory behavior are characteristics of AD, the open field test was utilized to further assess anxiety and exploration. The trajectories of the mice in the open field (Fig. 2E) indicated that, compared to controls, sh-GABRG2

mice spent significantly less time in the center and covered less distance overall ($p < 0.01$) (Fig. 2F).

Degradation of spatial memory and learning functions is among the most prominent behavioral changes in AD. Therefore, it was hypothesized that abnormal expression of GABRG2 might affect these cognitive functions in mice. This effect was assessed using the Y-maze and Morris water maze tests. In the Y-maze test, sh-GABRG2 mice showed a significantly lower alternation percentage than the control group ($p < 0.01$), though no significant difference was observed in the total number of arm entries ($p > 0.05$) (Fig. 2G). In the Morris water maze test, compared to controls, sh-GABRG2 mice exhibited an increased escape latency, decreased occupancy in the target quadrant, and fewer target crossings ($p < 0.01$), with no significant difference in total distance traveled ($p > 0.05$) (Fig. 2H).

Therefore, the knockdown of GABRG2 reduced social interactions, increased anxiety, diminished exploratory behavior, and impaired spatial memory and learning abilities in mice. These findings underscore the critical role of GABRG2 in regulating complex behaviors relevant to AD pathology.

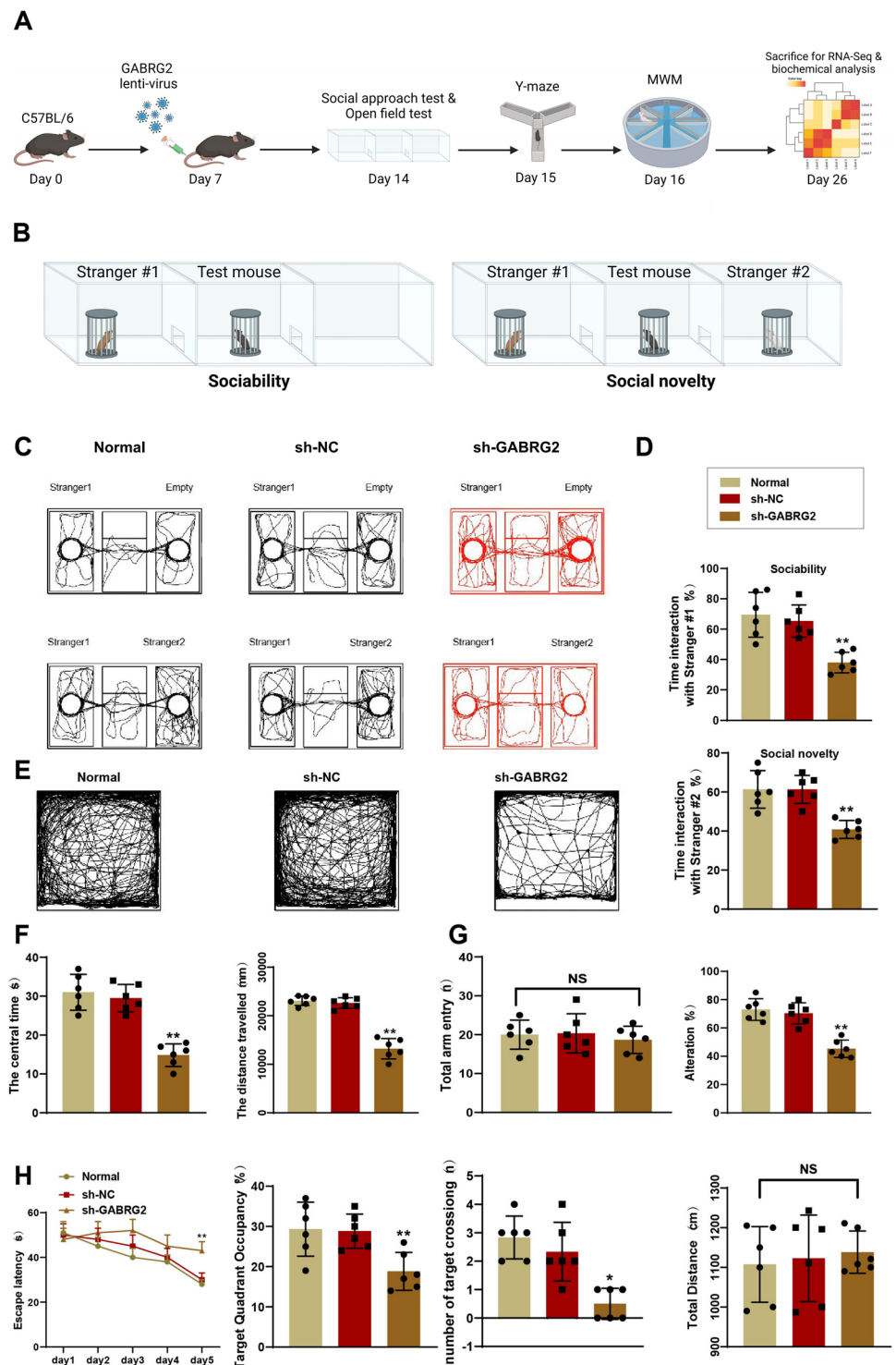
Impact of GABRG2 Silencing on GABAergic Neuron Functionality and GABA Expression

To confirm the effect of GABRG2 knockdown on the sh-GABRG2 group mice, the expression levels of GABRG2 protein in the frontal cortex tissues were initially assessed using Western blot. The results indicated a significant downregulation of GABRG2 protein expression in the sh-GABRG2 group compared to the control group ($p < 0.01$) (Fig. 3A). GABA, or γ -aminobutyric acid, serves as the primary inhibitory neurotransmitter in the central nervous system and is commonly implicated in the pathology of many central nervous system disorders [49].

Whole-cell patch-clamp recordings were conducted on neurons in brain slices from the frontal cortex of the model mice to examine the impact of GABRG2 on GABAergic neurons (Fig. 3B). We recorded GABA's mIPSCs and spontaneous inhibitory postsynaptic currents (sIPSCs). Representative traces of mIPSCs and sIPSCs from both sh-NC and sh-GABRG2 groups are shown in Fig. 3C. It was observed that both mIPSC and sIPSC amplitudes were significantly reduced in the sh-GABRG2 group ($p < 0.01$), whereas the differences in frequency were not statistically significant ($p > 0.05$) (Fig. 3D).

Immunofluorescent staining was performed on frozen brain slices to further validate the effects of GABRG2 expression changes on GABA levels. The results demonstrated a significant reduction in GABA-positive

Fig. 2 Effects of GABRG2 silencing on mouse social behavior, anxiety, spatial memory, and learning ability. **A** Workflow for establishing the GABRG2 knockdown mouse model and conducting behavioral tests using *in vivo* lentiviral transduction. **B** Schematic illustration of the three-chamber social interaction test. **C** Movement trajectory in the three-chamber social interaction test for mice in each group. **D** Bar chart showing the time spent in different chambers by mice in each group. **E** Movement trajectory in the open field test for mice in each group. **F** Bar chart showing the time spent in the center and total distance traveled in the open field test by mice in each group. **G** Bar chart showing the percentage of correct arm entries and total arm entries in the Y-maze spontaneous alternation test for mice in each group. **H** Bar chart showing the escape latency, target quadrant occupancy rate, the number of target crossings, and the total distance traveled in the Morris water maze test for mice in each group. $n = 6$. * $p < 0.05$, ** $p < 0.01$ compared to the sh-NC group. NS: $p > 0.05$. Data were compared using one-way ANOVA



expression in the frontal cortex of the sh-GABRG2 mice compared to controls. Statistical analysis of the positive ratios confirmed the significance of these differences ($p < 0.01$) (Fig. 3E–F). Consistent with the immunofluorescence results, the concentration of GABA in the cerebrospinal fluid (CSF) of the mice also showed a significant decrease

in the sh-GABRG2 group compared to the control group ($p < 0.01$) (Fig. 3G).

Collectively, these results demonstrated that silencing GABRG2 affected the electrophysiological activity of GABAergic neurons and concurrently reduced the levels of GABA expression, thereby substantiating the crucial

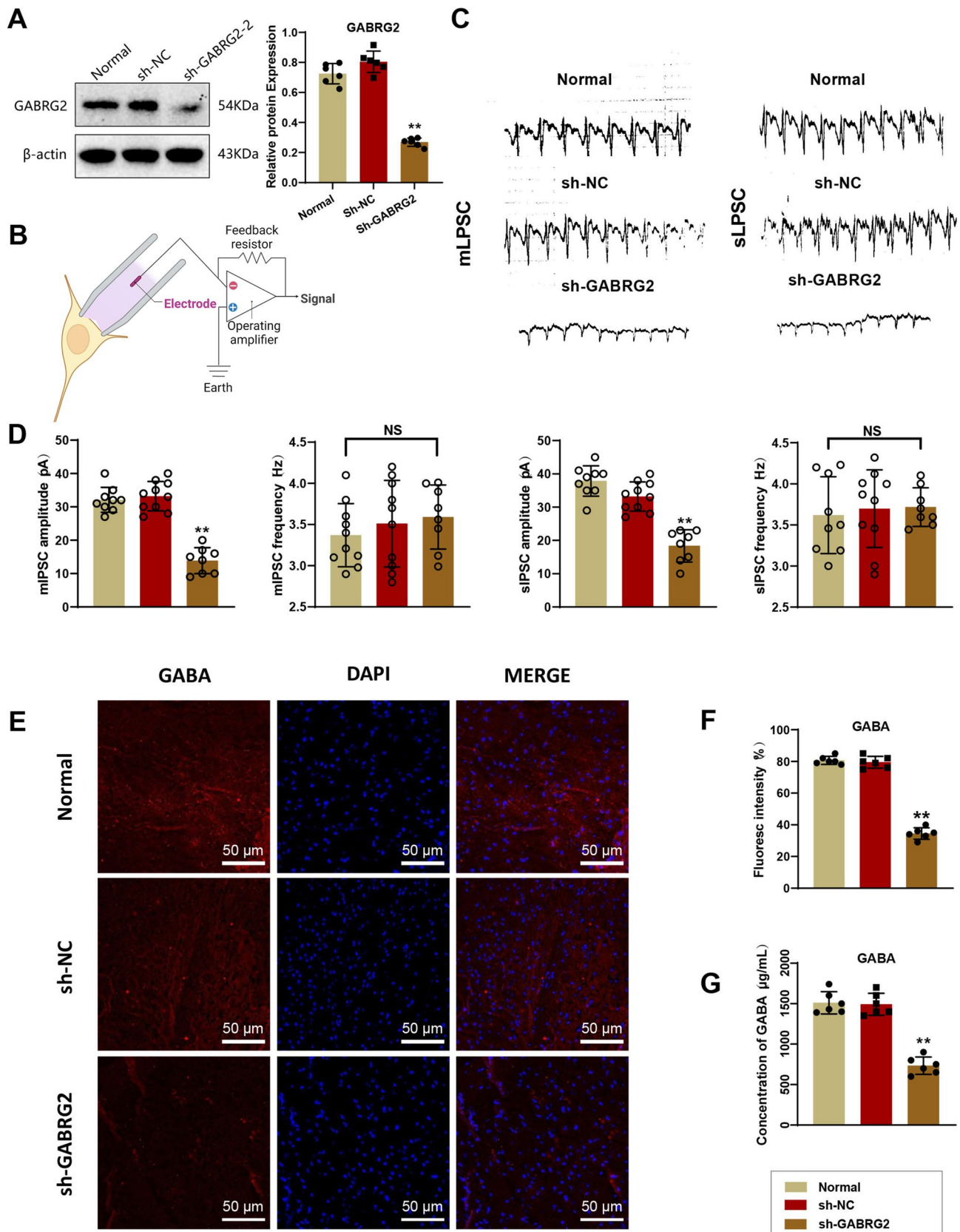


Fig. 3 Effects of GABRG2 silencing on GABAergic neuronal function and GABA expression in the frontal cortex of mice. **A** Western blot analysis to determine the efficacy of GABRG2 silencing in the frontal cortex tissue of mice. **B** Schematic diagram of whole-cell patch-clamp recording in neurons. **C** Representative traces of mIPSCs and sIPSCs in the frontal cortex neurons of mice in each group. **D** Bar chart showing the frequency and amplitude of mIPSCs and sIPSCs in the frontal cortex neurons of mice in each group. The number of cells in each group of brain slices was 9, 10, and 8, respectively. **E** Immunofluorescence staining to examine GABA expression in each group's frozen sections of the frontal cortex of mice. **F** Bar chart showing the percentage of immunofluorescence staining-positive area. **G** ELISA analysis of GABA concentration in the CSF of mice in each group. $n = 6$. * $p < 0.05$, ** $p < 0.01$ compared to the sh-NC group. NS: $p > 0.05$. Data were compared using one-way ANOVA. Bar = 50 μm

role of GABRG2 in regulating inhibitory neurotransmission and neuronal excitability.

rTMS Treatment Ameliorates Behavioral Deficits in 5xFAD Mice via GABRG2 Regulation

To assess the therapeutic effect of rTMS and its interaction with GABRG2 in AD, 5xFAD mice were utilized to simulate AD-like pathologies *in vivo*. These mice were subjected to rTMS treatments in the presence or absence of GABRG2 knockdown transduction (AD + rTMS group and AD + sh-GABRG2 + rTMS group, respectively) (Fig. 4A). The frequency and intervals of rTMS treatment are detailed in Fig. 4B.

Initially, the social interaction changes among the groups were evaluated using a three-chamber social interaction test. The results demonstrated a significant reduction in the duration of interaction with unfamiliar mice in the AD group compared to controls ($p < 0.01$). This interaction time was significantly restored under rTMS treatment compared to the AD group alone ($p < 0.01$). However, this improvement was notably reversed with the transduction of sh-GABRG2 ($p < 0.01$) (Fig. 4C–D).

An open-field test was conducted to assess anxiety and exploratory behaviors. The AD group mice displayed significantly reduced central zone occupancy and total walking distance compared to controls ($p < 0.01$). rTMS treatment increased both metrics compared to the AD group ($p < 0.01$), but these improvements were reversed by silencing GABRG2 ($p < 0.01$) (Fig. 4E–F).

Spatial memory and learning functions were evaluated using the Y-maze alternation test and the Morris water maze. In the Y-maze test, the percentage of alternation was significantly lower in the AD group compared to the WT group ($p < 0.01$). This percentage was restored in the

AD + rTMS group ($p < 0.01$), but the effect of rTMS was reversed following GABRG2 silencing. No significant differences were observed in the total number of arm entries across the groups ($p > 0.05$) (Fig. 4G).

In the Morris water maze, compared to controls, the AD group showed increased escape latency and reduced occupancy and crossings in the target quadrant ($p < 0.01$). Treatment with rTMS in the AD + rTMS group decreased escape latencies and increased occupancy and crossings compared to the AD group, with these differences being statistically significant ($p < 0.01$). However, these improvements were reversed when GABRG2 was silenced ($p < 0.01$). The total distance traveled did not differ significantly across the groups ($p > 0.05$) (Fig. 4H).

These findings indicate that rTMS can effectively mitigate behavioral alterations in 5xFAD mice and that its efficacy depends on the presence of GABRG2. The reversal of rTMS benefits following GABRG2 knockdown underscores the critical role of GABRG2 in the therapeutic modulation of AD-like behaviors by rTMS.

rTMS Mitigates Neuroinflammation and A β Deposition in 5xFAD Mice through Modulating GABRG2

Prior research suggests that rTMS treatment can alleviate neuroinflammation in AD, providing a basis for its application in AD therapy [50]. Hence, the study was furthered by examining the effects of rTMS on neuroinflammation and A β deposition and exploring whether these effects were GABRG2-dependent. We measured the expression of pro-inflammatory cytokines in the frontal cortex of mice using Western blot. Compared to the WT group, the expression of TNF- α , IL-1 β , and IL-6 was significantly upregulated in the AD group ($p < 0.01$). rTMS treatment significantly suppressed these pro-inflammatory markers ($p < 0.01$). However, this suppression was reversed when GABRG2 was silenced ($p < 0.01$) (Fig. 5A). RT-qPCR results confirmed these findings (Fig. 5B).

Furthermore, immunofluorescence staining was performed to assess A β deposition in the brain cortex of the mice. Compared to the WT group, a significant increase in the area of A β positive staining was observed in the AD group ($p < 0.01$). This increase was inhibited under rTMS treatment ($p < 0.01$), but the inhibition was reversed following GABRG2 silencing ($p < 0.01$) (Fig. 5C).

The results suggested that rTMS could alleviate neuroinflammation and reduce A β deposition in 5xFAD mice by affecting GABRG2.

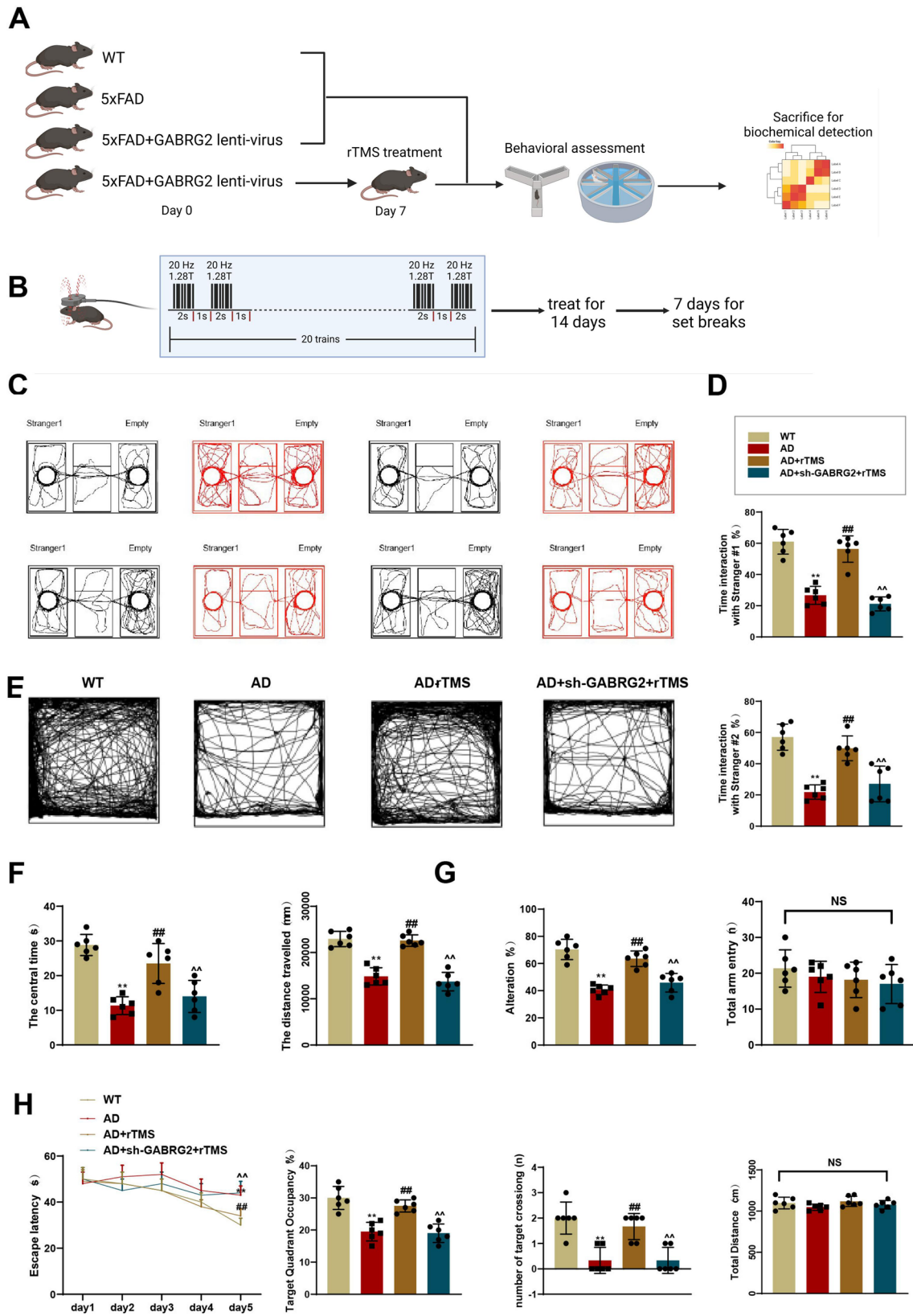


Fig. 4 Effects of rTMS treatment and sh-GABRG2 on behavioral changes in 5xFAD mice. **A** Workflow for the experimental procedures involving rTMS treatment and sh-GABRG2 in 5xFAD mice. **B** Schematic illustration of the rTMS treatment. **C** Movement trajectory in the three-chamber social interaction test for mice in each group. **D** Bar chart showing the time spent in different chambers by mice in each group during the three-chamber social interaction test. **E** Movement trajectory in the open field test for mice in each group. **F** Bar chart showing the time spent in the center and total distance traveled in the open field test by mice in each group. **G** Bar chart showing the percentage of correct arm entries and total arm entries in the Y-maze spontaneous alternation test for mice in each group. **H** Bar chart showing the escape latency, target quadrant occupancy rate, the number of target crossings, and the total distance traveled in the Morris water maze test for mice in each group. $n = 6$. * $p < 0.05$, ** $p < 0.01$ compared to the WT group. # $p < 0.05$, ## $p < 0.01$ compared to the AD group. ^ $p < 0.05$, ^^ $p < 0.01$ compared to the AD + rTMS group. NS: $p > 0.05$. Data were compared using an unpaired t test

rTMS Enhances GABAergic Neuronal Function and GABA Expression in 5xFAD Mice via the Regulation of GABRG2

GABA is the main inhibitory neurotransmitter in the central nervous system. Previous studies have documented a noticeable reduction and remodeling of GABA signaling in AD cases, which correlates with reduced inhibitory capacity and increased excitability in various cortical areas of the AD brain, as well as with the degree of dementia [51].

In our study, transcriptome sequencing analysis of subjects treated with rTMS revealed abnormalities in the gene encoding the GABA_{AR} γ subunit, GABRG2. Observations in the GABRG2 knockdown model indicated impaired functionality of GABAergic neurons, specifically shown by the reduced amplitude of sIPSCs and mIPSCs. This finding led to the hypothesis that rTMS could improve GABAergic neuron functionality by acting on GABRG2. To test this hypothesis, sIPSCs and mIPSCs of neurons in the frontal cortex of the mice were measured. Representative waveforms of sIPSCs and mIPSCs from the various groups are displayed (Fig. 6A).

Statistical analysis revealed that the amplitude of sIPSCs and mIPSCs significantly decreased in the AD group compared to the control group ($p < 0.01$) and was restored under rTMS treatment ($p < 0.01$). However, this restoration effect was reversed when GABRG2 was silenced ($p < 0.01$). No significant differences in the frequency of sIPSCs and mIPSCs were observed between the groups ($p > 0.05$) (Fig. 6B).

Finally, the expression of GABA in the frontal cortex was examined. Immunofluorescent staining results indicated that GABA expression was significantly weakened in the AD group compared to the WT group. This reduction was alleviated by rTMS treatment; however, the alleviation was reversed after GABRG2 silencing (Fig. 6C–D). The GABA concentration measurements in CSF were consistent with these findings (Fig. 6E).

Our results suggested that rTMS treatment might improve the impaired functionality of GABAergic neurons and the reduced expression levels of GABA in 5xFAD mice through the modulation of GABRG2.

GABRG2 Modulates SNAP25 Expression to Affect Synaptic Functions in 5xFAD Mice

The transcriptomic sequencing was conducted on the frontal cortex tissues of GABRG2-silenced mice and their controls to investigate the potential mechanisms of GABRG2. This analysis identified 4142 DEGs (Fig. 7A). These DEGs were intersected with DEGs identified in rTMS-treated and untreated mice (Fig. 1A), yielding 130 key genes (Fig. 7B). Further, GO functional analysis was applied to these genes based on a p -adjust < 0.05 . The top 20 entries in the GO analysis pertained to cellular components, such as glutamatergic synapse and presynaptic membrane, and biological processes, including synaptic transmission and GABAergic activity (Fig. S3A–D, Fig. 7C). SNAP25 was identified with the most interactions in the PPI network constructed from these 130 DEGs (Fig. 7D–E). SNAP25, a crucial component of the SNARE complex involved in neurotransmitter release at synapses was closely associated with vesicle docking, transport, and secretion (Fig. 7F).

We further validated our bioinformatics findings *in vivo*. RT-qPCR showed a significant downregulation of SNAP25 mRNA in the GABRG2-silenced group compared to controls ($p < 0.01$), and the Western blot analysis indicated a significant downregulation of SNAP25 protein levels in the sh-GABRG2 group ($p < 0.01$) (Fig. 7G–H). The immunohistochemical staining revealed a significant reduction in SNAP25 positive staining area in the GABRG2-silenced mice's frontal cortex ($p < 0.01$) (Fig. 7I). These findings suggested that SNAP25 expression was regulated by GABRG2, thus potentially affecting AD-like changes in mice through modulation of vesicular proteins and synaptic functions.

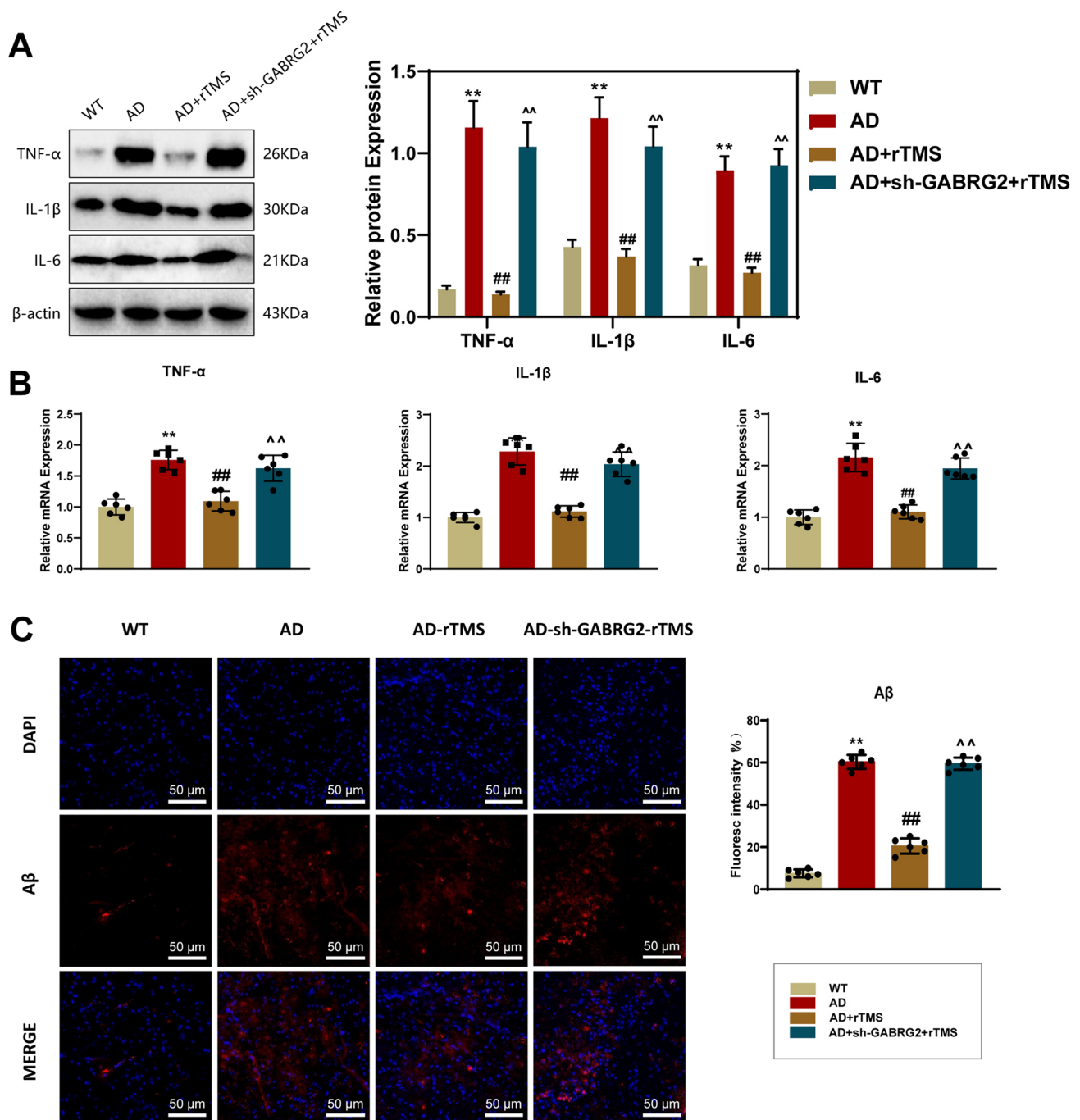


Fig. 5 Effects of rTMS treatment and sh-GABRG2 on neuroinflammation and A β deposition in 5xFAD mice. **A** The expression levels of TNF- α , IL-1 β , and IL-6 in the frontal cortex protein of mice in each group were detected by Western blot. **B** The expression levels of TNF- α , IL-1 β , and IL-6 in the frontal cortex mRNA of mice in each group were detected by RT-qPCR. **C** The expression of A β in the cor-

tical tissue and the statistical column chart of fluorescence area ratio in the brains of mice in each group were detected by immunofluorescence staining. $n = 6$. * $p < 0.05$, ** $p < 0.01$ compared with the WT group; # $p < 0.05$, ## $p < 0.01$ compared with the AD group; ^ $p < 0.05$, ^^ $p < 0.01$ compared with the AD + rTMS group. Data were compared using an unpaired t test. Bar = 50 μ m

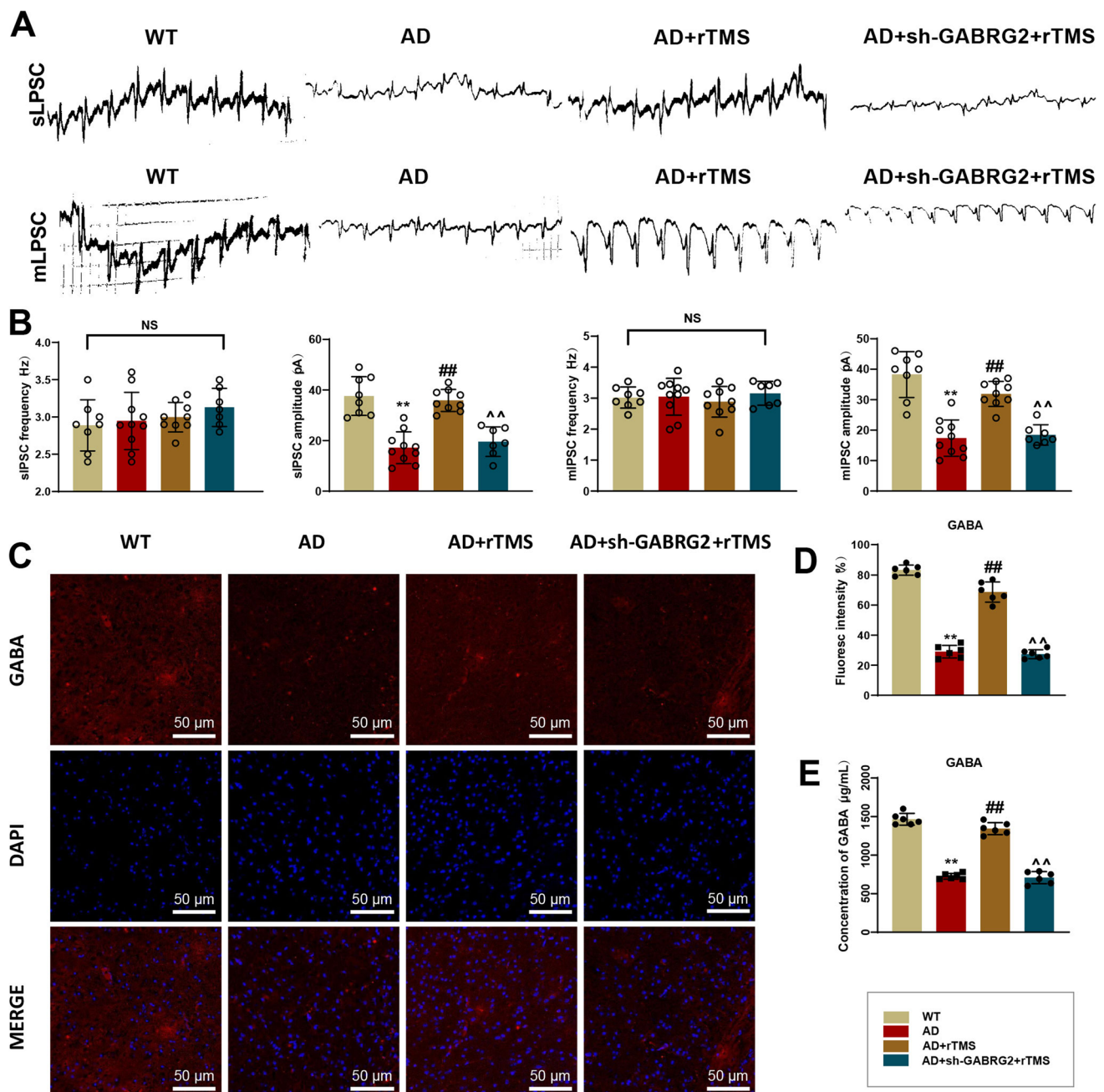


Fig. 6 Effects of rTMS treatment and sh-GABRG2 on GABAergic neuronal electrophysiology, GABA expression levels, and GABA concentration in the CSF of 5xFAD mice. **A** Typical traces of mIPSCs and sIPSCs of neurons in the frontal cortex of mice in different groups. **B** Statistical column chart of the frequency and amplitude of mIPSCs and sIPSCs of neurons in the frontal cortex of mice in different groups, with a total of 8, 10, 9, and 8 brain slices for each group. **C** The expression of GABA in the frontal cortex of mice in differ-

ent groups was detected by immunofluorescence staining. **D** Statistical column chart of the proportion of GABA-positive fluorescence area obtained from immunofluorescence staining. **E** The concentration of GABA in the CSF of mice in different groups was detected by ELISA. $n = 6$. * $p < 0.05$, ** $p < 0.01$ compared with the WT group; # $p < 0.05$, ## $p < 0.01$ compared with the AD group; ^ $p < 0.05$, ^^ $p < 0.01$ compared with the AD + rTMS group. Data were compared using an unpaired t test. Bar = 50 µm

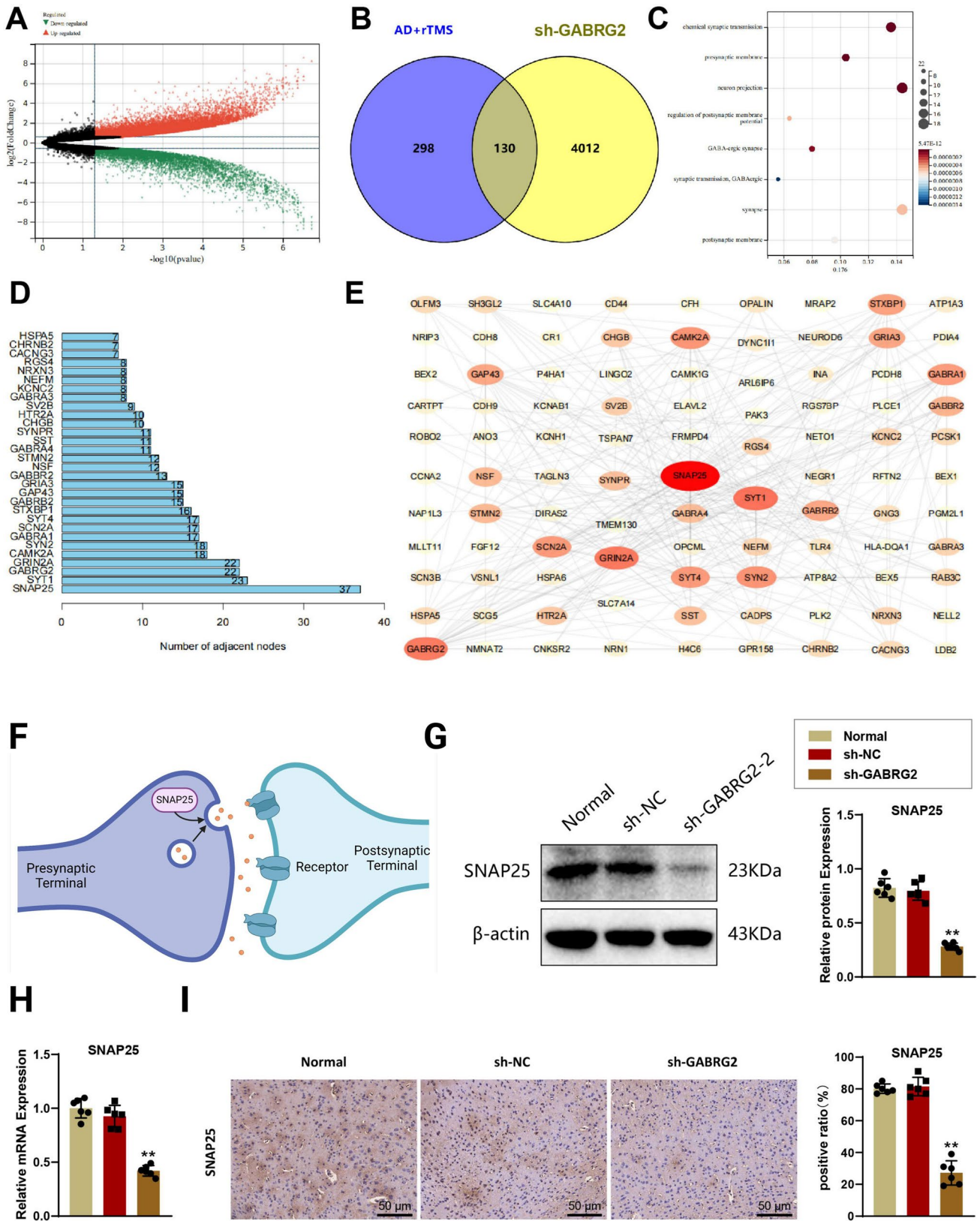


Fig. 7 Further exploration of downstream key signals regulated by GABRG2. **A** Volcano plot of DEGs in the transcriptome sequencing of the frontal cortex samples from mice in each group. **B** Venn diagram showing the intersection of DEGs in the transcriptome sequencing of the frontal cortex samples from AD patients receiving or not receiving rTMS treatment and mice in the AD + rTMS + sh-GABRG2 or AD + sh-GABRG2 groups. **C** Bubble plot showing the GO enrichment results of 130 target genes. **D–E** PPI network of the 130 candidate genes is based on the STRING database and visualized using Cytoscape software, with darker colors and larger circles representing higher degree values. **F** Schematic diagram illustrating the mechanism of action of SNAP25 downstream genes in synaptic transmission in neurons. **G** The protein levels of SNAP25 in the frontal cortex tissue of mice in different groups were detected by Western blot. **H** The mRNA levels of SNAP25 in the frontal cortex tissue of mice in different groups were detected by RT-qPCR. **I** The expression of SNAP25 in the frontal cortex tissue of mice in different groups was detected by immunohistochemistry. * $p < 0.05$, ** $p < 0.01$ compared with the WT group; # $p < 0.05$, ## $p < 0.01$ compared with the AD group; ^ $p < 0.05$, ^^ $p < 0.01$ compared with the AD + rTMS group. $n = 6$. Data were compared using an unpaired t test. Bar = 50 μm

rTMS Restores Synaptic Functions in Mice with AD-Like Phenotypes by Modulating Vesicle-Associated Protein Expression via GABRG2 Regulation

The SNARE complex, comprising three alpha-helical proteins including SNAP25, syntaxin, and vesicle-associated membrane protein (VAMP), is essential in neurotransmitter release at presynaptic membranes, with synaptotagmin-1 (SYT1) regulating this process as a presynaptic calcium sensor (Fig. 8A). Synaptic loss and dysfunction are recognized as central features of AD, which confer crucial roles in the progression and manifestation of behavioral and physiological symptoms. These aspects are pivotal in exploring the pathogenesis and therapeutic approaches of AD [52]. Hence, we hypothesized that rTMS might influence synaptic function by regulating the expression of vesicular proteins through GABRG2.

To test this hypothesis, Western blot analysis was used to measure the expression of SNAP25, SYT1, and VAMP-2 in the frontal cortex tissues of mice. Compared to the control group, the expression of these proteins was significantly downregulated in the AD group ($p < 0.01$). rTMS treatment led to an upregulation of these proteins ($p < 0.01$), which was reversed upon GABRG2 silencing ($p < 0.01$) (Fig. 8B). Immunohistochemical staining corroborated these findings (Fig. 8C).

The function of synapses was further assessed by measuring spike probability (Fig. 8D). Compared to controls, the spike probability was significantly reduced in the frontal cortex neurons of the AD group ($p < 0.01$). rTMS significantly increased the reduced spike probability in AD mice ($p < 0.01$), but this effect was reversed when GABRG2 was silenced ($p < 0.01$) (Fig. 8E–F).

These results indicated that rTMS might modulate the expression of vesicular proteins and affect synaptic function by regulating GABRG2 expression, thereby potentially alleviating the neurological symptoms associated with AD in 5xFAD mice.

Overexpression of SNAP25 Modulates Vesicle-Associated Proteins and Enhances Synaptic Function in the Context of rTMS and GABRG2 Silencing in Mice with AD-Like Phenotypes

In preliminary studies, the key gene SNAP25, which is closely related to GABRG2, was identified as exhibiting expression differences in GABRG2-silenced mice. Additionally, the modulation of vesicular protein expression and synaptic function by rTMS-GABRG2 was observed. Given SNAP25's critical role in vesicle transport as part of the SNARE complex, we explored its involvement in regulating other vesicular proteins and synaptic functions. Abnormal expression of SNAP25 affects the expression of other SNARE complex components, vesicle transport, neurotransmitter release, and synaptic function [53]. We hypothesized that under the influence of rTMS, GABRG2 could further modulate SNAP25 to orchestrate vesicular protein expression and synaptic function.

To validate this hypothesis, SNAP25 was ectopically expressed in mice subjected to GABRG2 silencing and rTMS treatment. With the AD + sh-GABRG2 + rTMS group as a control, we further explored the role of SNAP25 as a downstream key gene in the mechanism where rTMS modulated GABRG2 to protect against AD. The expression levels of vesicular proteins SNAP25, SYT1, and VAMP-2 in the frontal cortex tissues of the two mouse groups were measured by Western blot. Compared to the AD + sh-GABRG2 + rTMS group, overexpression of SNAP25 significantly upregulated the expression levels of SNAP25, SYT1, and VAMP-2 ($p < 0.01$) (Fig. 9A).

Consistent results were obtained via RT-qPCR ($p < 0.01$) (Fig. 9B). Immunohistochemical staining demonstrated that in the AD + sh-GABRG2 + OE-SNAP25 + rTMS group, the area of positive staining for SNAP25, SYT1, and VAMP-2 in the frontal cortex was significantly increased compared to the control group, with statistically significant differences in positive area ratio ($p < 0.01$) (Fig. 9C).

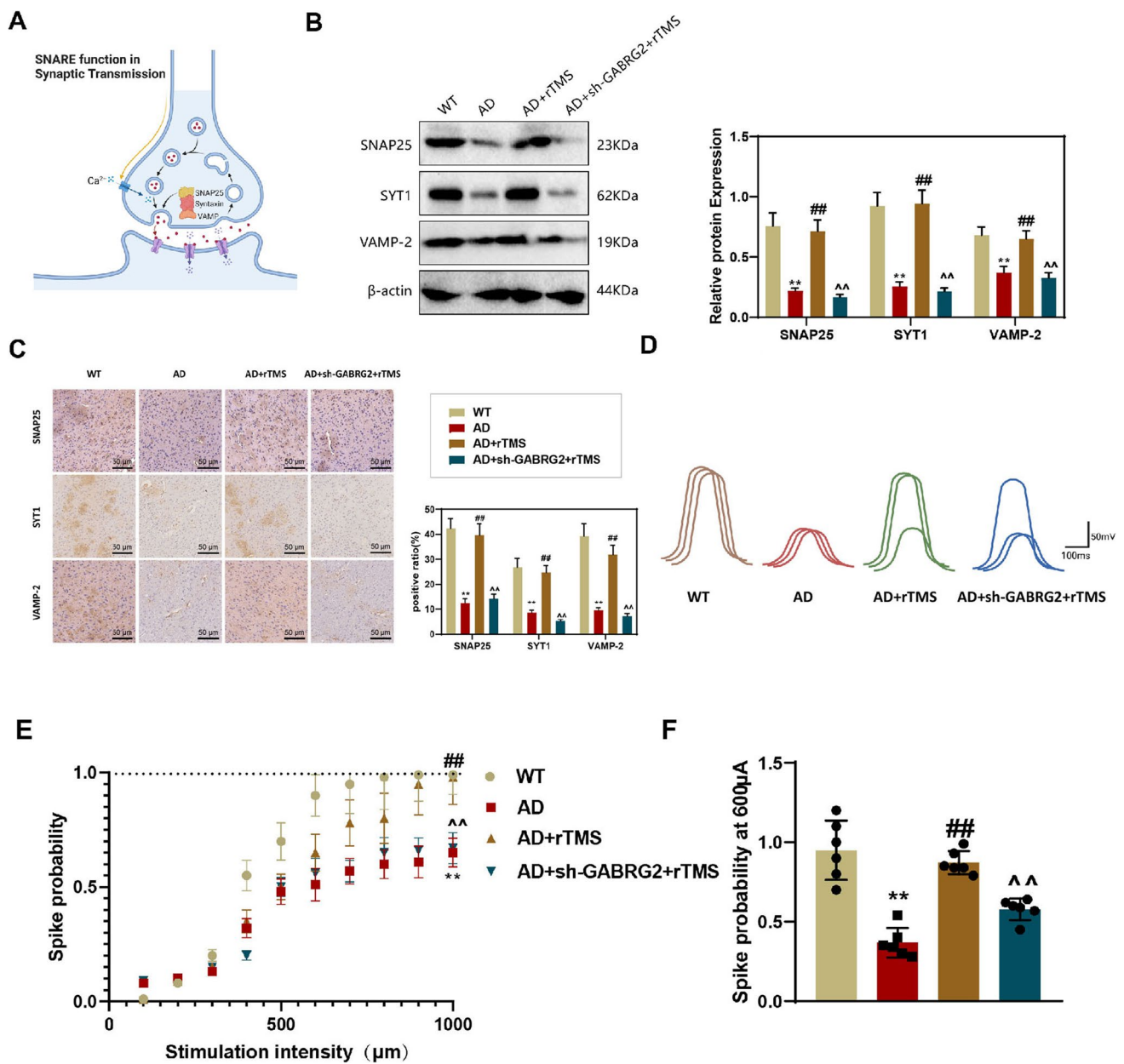


Fig. 8 Effects of SNAP25 silencing on vesicle protein and peak probability. **A** Schematic diagram showing the role of SNAP25 and vesicle-related proteins in vesicle transport and neurotransmitter release. **B** The expression levels of vesicle-related proteins after SNAP25 silencing were detected by Western blot. **C** The expression levels of vesicle-related proteins in the frontal cortex tissue of mice after SNAP25 silencing were detected by immunohistochemistry. **D**

Representative tracing images of peak probability determination in the frontal cortex of mice in each group. **E** Quantification of the peak probability. **F** Quantification of the peak probability with 600 μ A stimulation. * $p < 0.05$, ** $p < 0.01$ compared with the WT group; # $p < 0.05$, ## $p < 0.01$ compared with the AD group; ^ $p < 0.05$, ^^ $p < 0.01$ compared with the AD + rTMS group. $n = 6$. Data were compared using an unpaired t test. Bar = 50 μ m

Further, the synaptic function of the two groups was evaluated by measuring spike probability, with representative traces shown in (Fig. 9D). Compared to the control group, mice with overexpressed SNAP25 exhibited significantly higher spike probability in neurons of the frontal cortex ($p < 0.01$) (Fig. 9E–F).

The results above uncovered that rTMS regulated the expression of SNAP25 and synaptic function via GABRG2, thereby affecting the expression of vesicle-associated proteins.

SNAP25 Overexpression Enhances rTMS-Induced Behavioral Improvements in GABRG2-Silenced Mice with AD-Like Phenotypes

These findings underscore the crucial role of SNAP25 in the modulation of vesicular proteins and synaptic function influenced by rTMS-GABRG2. Further, we evaluated behavioral changes in the mouse groups to assess the effectiveness of rTMS treatment in alleviating AD symptoms by regulating SNAP25 under reduced GABRG2 expression. In the three-chamber social interaction test, mice in the AD + sh-GABRG2 + OE-SNAP25 + rTMS group exhibited significantly increased interaction times with unfamiliar mice #1 and #2 compared to the AD + sh-GABRG2 + rTMS group ($p < 0.01$) (Fig. 10A–B).

In the open field test, mice with overexpressed SNAP25 spent more time in the center and traveled greater total distances compared to the target group, indicating significantly reduced anxiety ($p < 0.01$) (Fig. 10C–D). Spatial learning and memory capabilities were further tested through the Y-maze and Morris water maze experiments. Although there was no difference in total arm entries, the percentage of alternation was significantly increased in the AD + sh-GABRG2 + OE-SNAP25 + rTMS group compared to controls (Fig. 10E). In the Morris water maze, despite similar distances traveled ($p > 0.05$), the escape latency decreased, and the occupancy rate and crossings in the target quadrant significantly increased ($p < 0.01$), indicating improved spatial memory and learning function (Fig. 10F).

These results demonstrated that rTMS might alleviate neuroinflammation and A β deposition in 5xFAD mice by regulating SNAP25 through GABRG2, highlighting its therapeutic potential in modulating AD-related synaptic and behavioral changes.

Overexpression of SNAP25 Attenuates Neuroinflammation and A β Deposition in GABRG2-Silenced Mice with AD-Like Phenotypes Under rTMS Treatment

Previous findings revealed that rTMS significantly reduced the expression of pro-inflammatory cytokines and A β deposition in the frontal cortex of 5xFAD mice. This effect was inhibited by silencing GABRG2. Behavioral tests demonstrated that overexpression of SNAP25 could reverse the inhibitory effects of silenced GABRG2. The role of SNAP25 overexpression on typical AD pathologies, such as neuroinflammation and A β deposition, was assessed by examining the expression of pro-inflammatory cytokines in the frontal cortex tissues of mice using Western blot. The results indicated a significant downregulation of TNF- α , IL-1 β , and IL-6 in mice overexpressing SNAP25 compared to the AD + sh-GABRG2 + rTMS group ($p < 0.01$) (Fig. 11A). Consistent results were obtained at the mRNA level ($p < 0.01$) (Fig. 11B).

Subsequently, immunofluorescence staining was performed on frozen brain sections of the frontal cortex to evaluate A β deposition. The intense positive expression of A β observed in the AD + sh-GABRG2 + rTMS group was significantly weakened in the AD + sh-GABRG2 + OE-SNAP25 + rTMS group, with statistically significant differences in the percentage of positive staining area ($p < 0.01$) (Fig. 11C).

These results uncovered that rTMS might alleviate neuroinflammation and A β deposition in 5xFAD mice by regulating SNAP25 through GABRG2. This mechanism highlights the potential of targeted synaptic protein modulation in treating AD pathologies effectively.

Discussion

In recent years, AD has remained a focal point in neurodegenerative disease research, with its underlying mechanisms continuing to attract considerable scientific interest [54]. Among the treatments under investigation, non-invasive techniques such as rTMS have increasingly garnered attention from the scientific community [8–10, 55]. rTMS has demonstrated therapeutic potential across various neuropsychiatric disorders, standing out for its safety and modulability, although its application in AD is still in the early stages [56, 57].

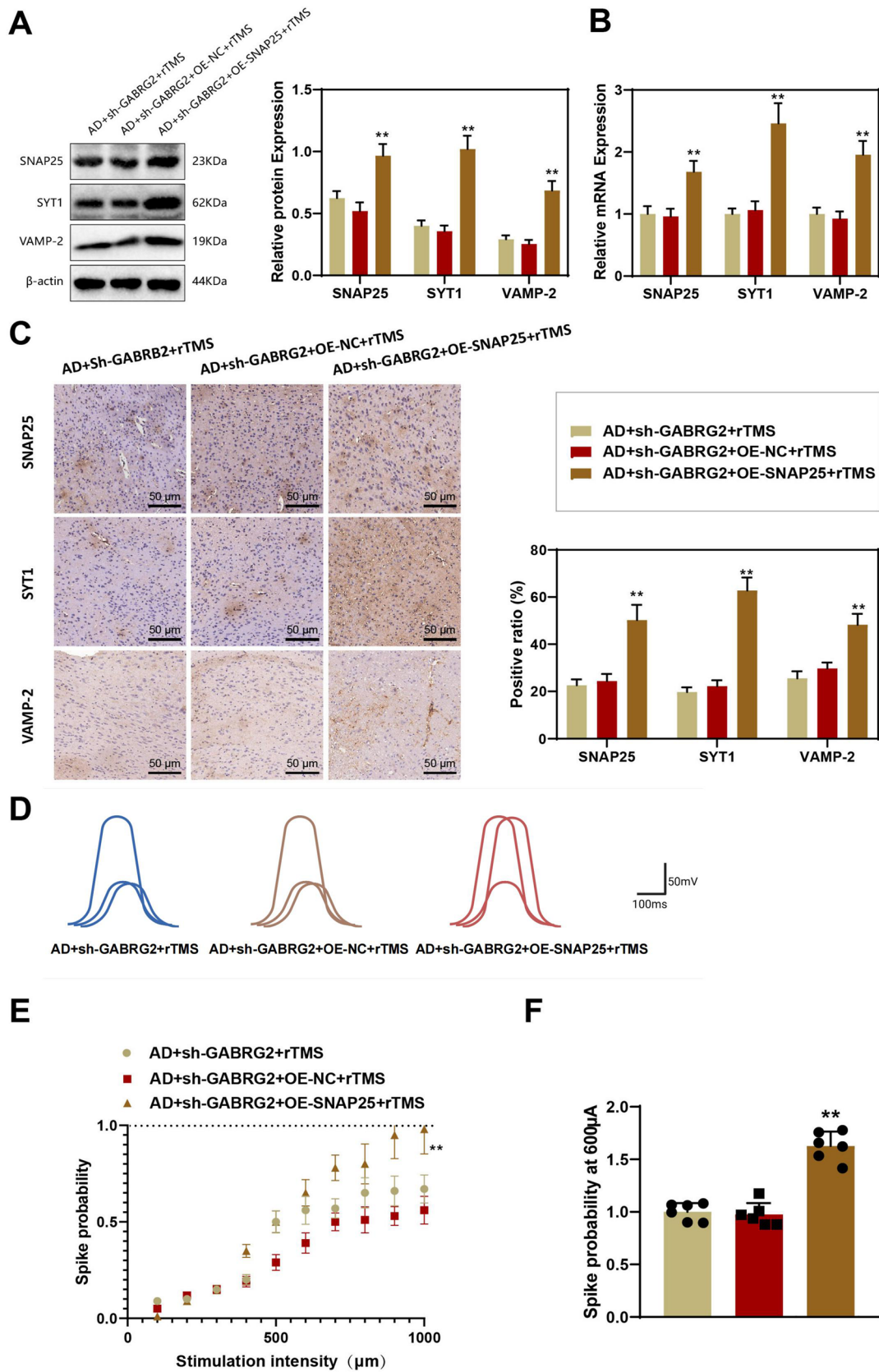


Fig. 9 Effects of SNAP25 on synaptic function in mice with AD-like phenotypes. **A** The expression levels of vesicle-related proteins in mice in each group were detected by Western blot. **B** RT-qPCR detected vesicle-related protein mRNA expression levels in mice in each group. **C** The expression of vesicle-related proteins in the frontal cortex of mice in each group was detected by immunohistochemistry. **D** Representative tracing images were used to display the results of peak probability determination in the frontal cortex of mice in each group. **E** Quantifying the peak probability with each group's 11, 9, and 15 observed cells. **F** Quantification of the peak probability with 600 μ A stimulation. * $p < 0.05$, ** $p < 0.01$ compared to the AD + sh-GABGR2 + rTMS group. $n = 6$. Data were compared using one-way ANOVA. Bar = 50 μ m

If proven effective for AD, rTMS would offer a safer, more acceptable treatment option for patients, emphasizing the importance of establishing concrete evidence of its efficacy and safety [11]. The findings of our study suggested that GABRG2 and SNAP25 could be new therapeutic targets in AD with potential treatment strategies. Given the complexity of AD pathology, a combination of various therapeutic approaches may enhance treatment efficacy. Future research should aim to verify these conclusions in human subjects, for example, through clinical trials testing rTMS in AD patients at different stages of the disease to confirm its efficacy and safety. Additionally, further studies should explore the optimal frequencies, intensities, and durations of rTMS treatment to achieve the best therapeutic outcomes.

Previous research has primarily focused on the general effects of rTMS on the nervous system rather than its specific molecular and cellular mechanisms [58]. For instance, early studies highlighted that rTMS can increase the excitability of diaphragmatic motor neurons through localized GABAergic “disinhibition” [59]. Our study advances this field by applying multi-omics techniques to delve into the molecular mechanisms of rTMS in AD [60]. We identified GABRG2 as a potential key target in rTMS treatment for AD. rTMS was observed to restore decreased amplitudes of spontaneous and miniature inhibitory postsynaptic currents (sIPSC and mIPSC) and GABA expression, improve impaired GABAergic neuron function, and enhance the expression of downregulated vesicular proteins. These changes significantly increased reduced spike probabilities and improved synaptic function. However, reversal experiments involving the silencing of GABRG2 indicated that these therapeutic effects could be undone, underscoring the crucial role of GABRG2 in mediating the benefits of

rTMS. This finding suggests a new direction for the in-depth application of rTMS, highlighting its potential to modulate specific molecular targets more precisely than previously understood.

GABRG2 plays a crucial role in neuronal activity [22], and its dysfunction is linked to various neurological disorders. Yet, its role in AD remains unclear [61]. Our research reveals its significant role in AD and, through multi-omics approaches, suggests a potential interaction with SNAP25. Immunohistochemical staining showed that the cortical SNAP25 positive staining area significantly decreased in sh-GABRG2 group mice, indicating that SNAP25 expression is regulated by GABRG2.

Furthermore, SNAP25 is a critical molecule for synaptic function, and its dysfunction can lead to various neurofunctional disorders [62]. Research indicates that the survival of glutamatergic and GABAergic neurons, dendritogenesis, and synaptic amplitude modulation require the coordinated release of SNAP-25a/b [63]. Our findings suggest that rTMS may affect SNAP25 through GABRG2 to achieve therapeutic effects in AD. Ectopic expression of SNAP25, following the silencing of GABRG2 and rTMS treatment, could restore the therapeutic effects of rTMS, providing new insights into the application of SNAP25 in the treatment of neurodegenerative diseases.

Our results preliminarily conclude that rTMS may improve GABAergic neuron function and enhance GABA expression, which is typically downregulated in AD. This enhancement further influences SNAP25 and regulates vesicular proteins to protect synaptic function, thereby alleviating AD symptoms. This study reveals a potential mechanism by which rTMS, through GABRG2, regulates SNAP25 (Fig. 12), providing a new perspective on AD pathophysiology.

This research primarily utilizes the 5xFAD mouse model, which, while rapidly developing AD-related neuropathological behavior, presents notable differences from humans, potentially limiting the direct applicability of the findings to human cases. The 5xFAD mice exhibit variability in the severity and consistency of learning and memory impairments across different studies. Notably, learning deficits manifest between 6 and 9 months of age but become more pronounced and confounded with motor impairments by 12–15 months [64]. The research into rTMS treatment for AD is still in its early stages, and more empirical evidence and long-term follow-up data are essential. rTMS may

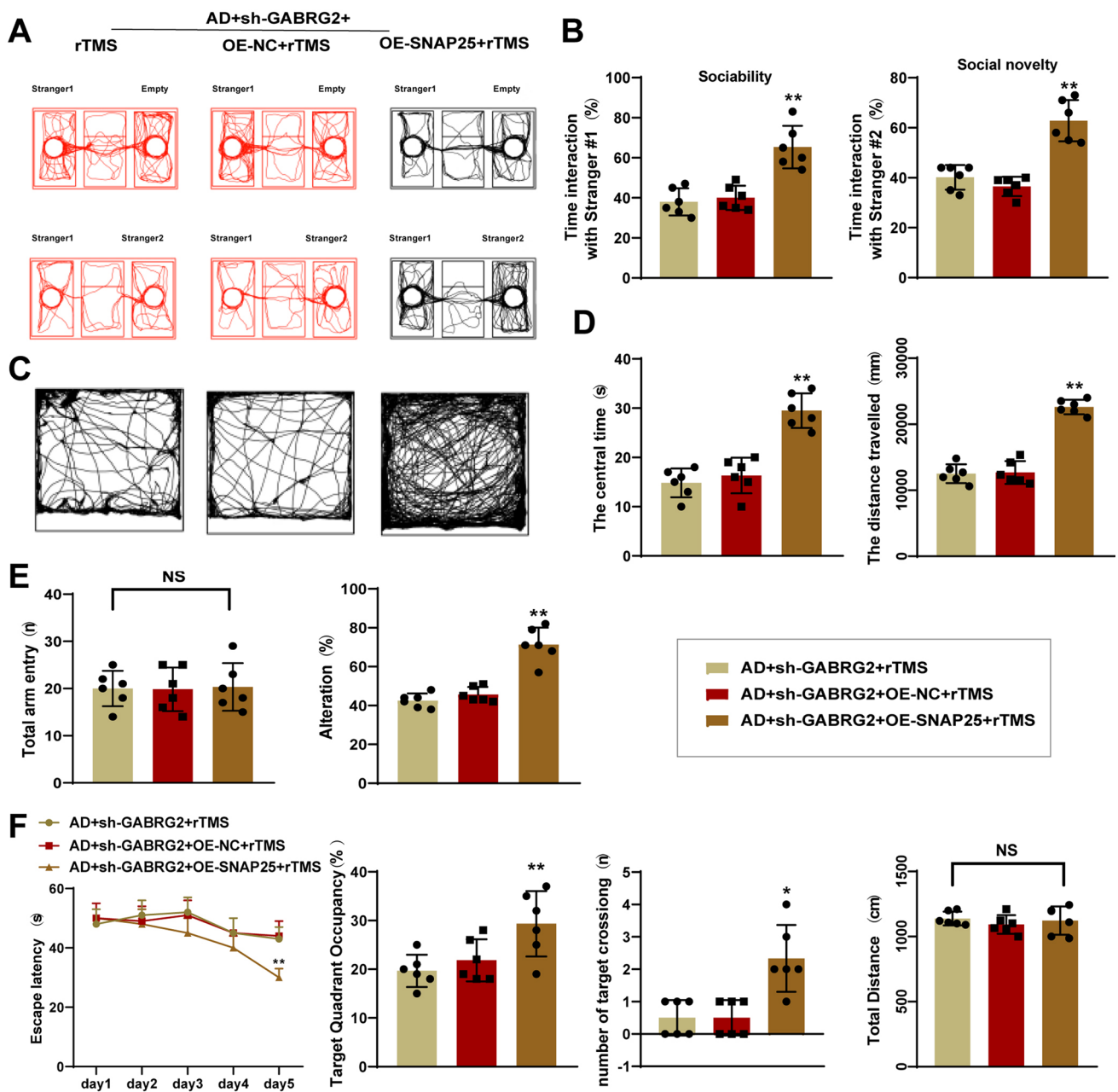


Fig. 10 Impact of SNAP25 overexpression on behavioral changes in rTMS-treated mice with AD-like phenotypes. **A** Track maps of mice in the three-chamber social interaction test for each group. **B** Bar graph showing the duration of stay in the three-chamber social interaction test for each group. **C** Track maps of mice in the open field test for each group. **D** Bar graph showing the duration of stay and total travel distance in the open field test for each group. **E** Bar

graph showing the percentage of arm entries and total arm entries in the Y-maze alternation test for each group. **F** Bar graphs showing the escape latency, target zone occupancy, number of target crossings, and total travel distance in the Morris water maze for each group. * $p < 0.05$, ** $p < 0.01$ compared to the AD + sh-GABGR2 + rTMS group. $n = 6$. Data were compared using one-way ANOVA

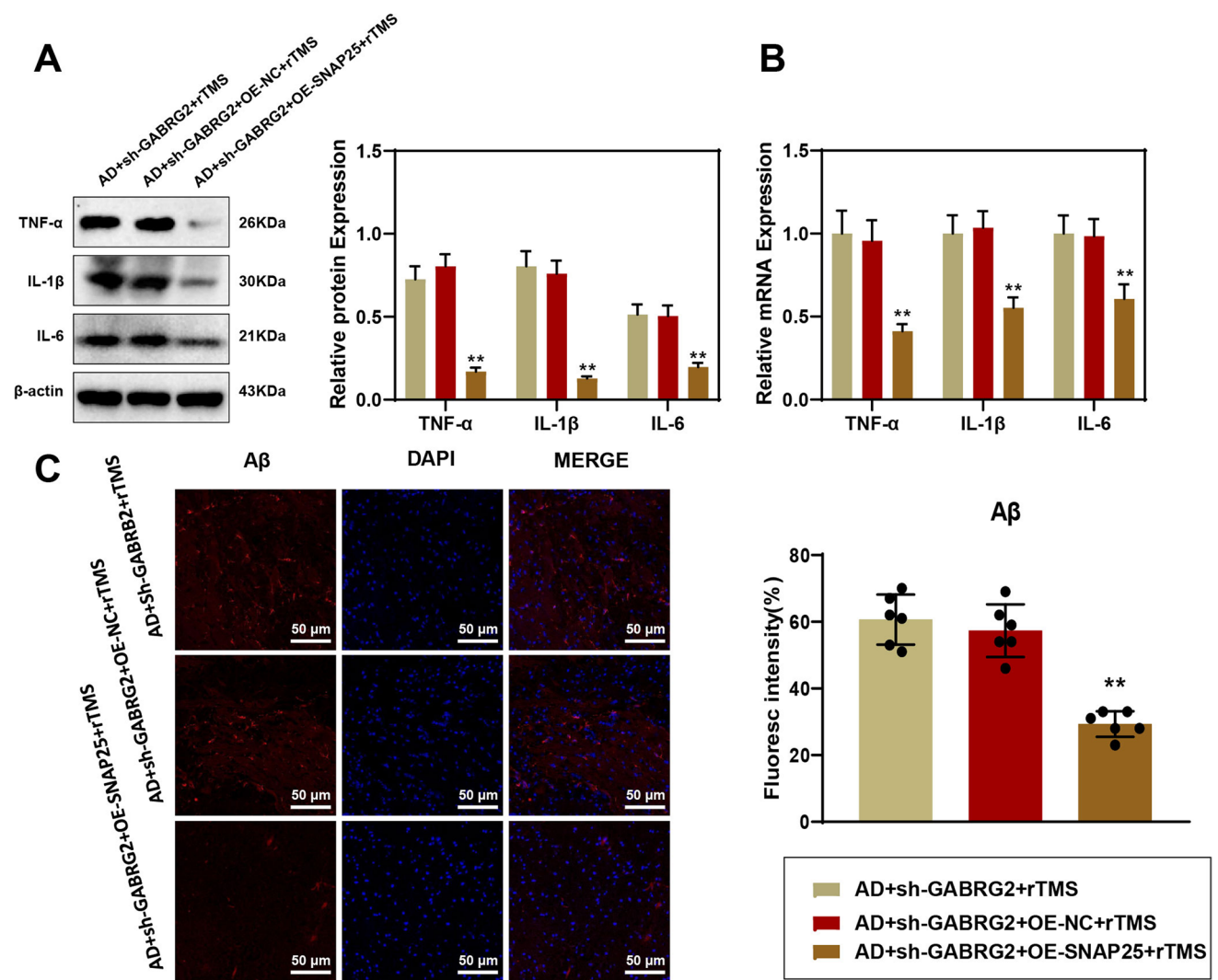


Fig. 11 The impact of SNAP25 overexpression on AD neuroinflammation and A β deposition. **A** Expression levels of pro-inflammatory cytokines in the prefrontal cortical tissue of mice from each group detected by Western blot. **B** Expression levels of pro-inflammatory cytokine mRNA in the prefrontal cortical tissue of mice from each

group detected by RT-qPCR. **C** Immunofluorescence staining showing the expression of A β in the prefrontal cortical tissue of mice from each group and bar graph of the positive fluorescence area. * $p < 0.05$, ** $p < 0.01$ compared to the AD + sh-GABGR2 + rTMS group. $n = 6$. Data were compared using one-way ANOVA

influence multiple pathways and mechanisms within the brain, potentially leading to nonspecific effects that could interfere with the study outcomes.

Future research should validate these findings in human patients through clinical trials that test rTMS on AD patients at various stages of disease progression to verify its efficacy and safety in humans. Clinical trials have demonstrated that, compared to a sham group, patients undergoing rTMS treatment show modest but significant cognitive improvements after 6 weeks, as assessed by the Mini-Mental State Examination and AD cognitive

assessments [65]. Moreover, the application of rTMS to bilateral AG has been shown to effectively improve AD-related neuropsychiatric symptoms, cognitive function, and sleep quality, with considerable safety [66]. Beyond the current focus, rTMS may also affect other pathways and mechanisms related to AD, meriting further investigation. Future studies should explore the optimal rTMS treatment frequency, intensity, and duration to achieve the best therapeutic outcomes. Given the complexity of AD, a combination of multiple treatment modalities may prove more effective. rTMS could be integrated with other

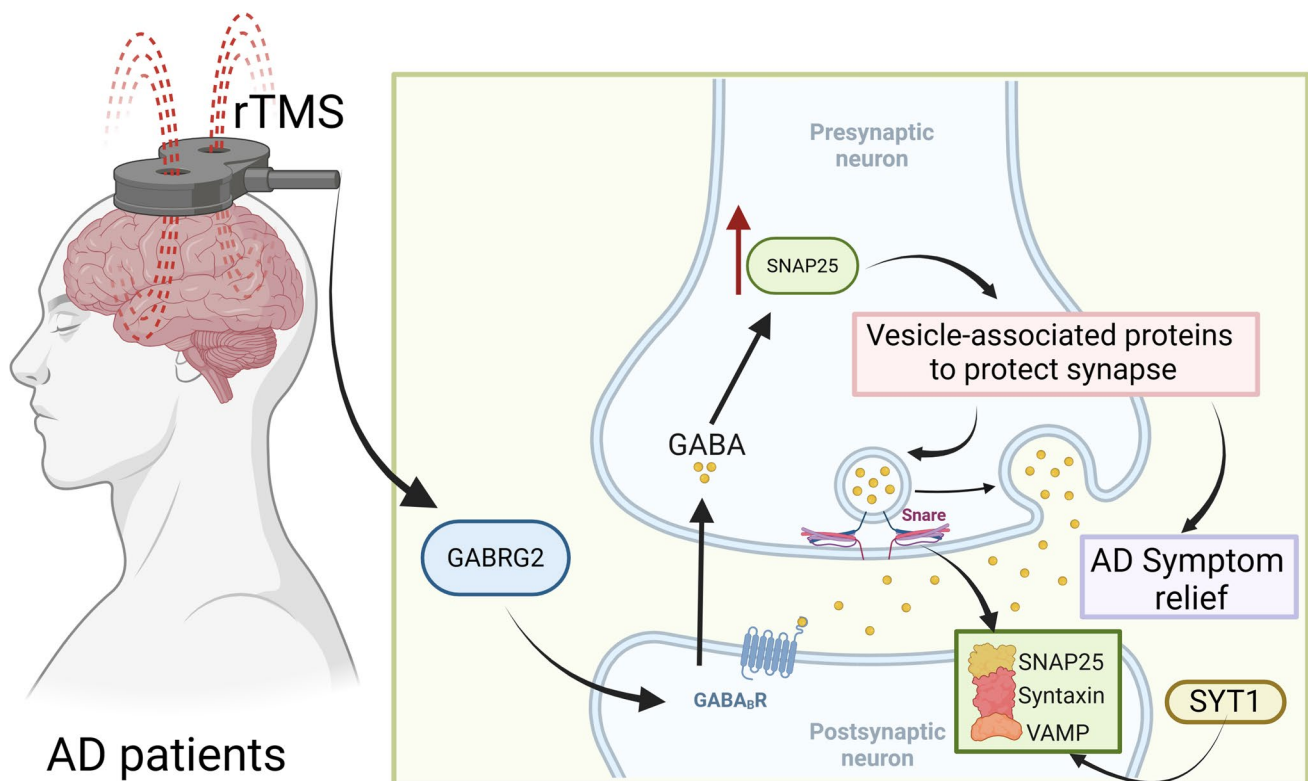


Fig. 12 Schematic diagram of the synaptic functional molecular mechanism through GABRG2-GABA-SNAP25 mediated by rTMS

pharmacological or non-pharmacological treatments to enhance its therapeutic effects.

In summary, this study provides preliminary evidence of the potential value of rTMS in the treatment of AD, yet further research is needed to validate and refine this method fully. The implications of our findings are promising, suggesting new therapeutic avenues for AD that could improve the quality of life for many affected individuals.

Supplementary Information The online version contains supplementary material available at <https://doi.org/10.1007/s12035-024-04354-7>.

Author Contribution JW: conceptualization, methodology, data curation; CZ: validation, visualization, investigation; ZH: formal analysis, resources, supervision; XJ: writing—original draft, funding acquisition; RC: data collection, statistical analysis; YK: project administration, manuscript review; GZ: experimental design, data interpretation; YW: writing—review and editing, manuscript preparation; TZ: literature review, ethical compliance.

Funding This study was supported by the Hebei Medical Science Research Project Plan (20240255), Hebei Provincial Natural Science Foundation Precision Medicine Joint Fund Cultivation Project (H2021206269, H2022206023), and Scientific Research Projects of Higher Education Institutions in Hebei Province (QN2024035).

Data Availability All data provided in this study are available from the corresponding author upon a reasonable requirement.

Declarations

Ethical Approval All experiments involving mice were approved by the Animal Ethics Committee of Hebei Medical University (IACUC-Hebmu-2023054).

Consent to Participate Not applicable.

Consent for Publication Not applicable.

Competing interests The authors declare no competing interests.

References

- Jeong HH, Chandrakantan A, Adler AC (2021) Obstructive sleep apnea and dementia—common gene associations through network-based identification of common driver genes. *Genes* 12(4):542. <https://doi.org/10.3390/genes12040542>
- Steininger G, Kostev K (2020) The role of the treating practice in persistence among dementia patients in Germany and the UK. *Int J Clin Pharmacol Ther* 58(5):247–253. <https://doi.org/10.5414/CP203670>
- Ranson JM, Rittman T, Hayat S, Brayne C, Jessen F, Blennow K, van Duijn C, Barkhof F, Tang E, Mummery CJ, Stephan BCM, Altomare D, Frisoni GB, Ribaldi F, Molinuevo JL, Scheltens P, Llewellyn DJ, European Task Force for Brain Health Services

- (2021) Modifiable risk factors for dementia and dementia risk profiling: A user manual for Brain Health Services-part 2 of 6. *Alzheimers Res Ther* 13(1):169. <https://doi.org/10.1186/s13195-021-00895-4>
4. Monteiro AR, Barbosa DJ, Remião F, Silva R (2023) Alzheimer's disease: insights and new prospects in disease pathophysiology, biomarkers and disease-modifying drugs. *Biochem Pharmacol* 211:115522. <https://doi.org/10.1016/j.bcp.2023.115522>
 5. Yang G, Seok JK, Kang HC, Cho YY, Lee HS, Lee JY (2020) Skin barrier abnormalities and immune dysfunction in atopic dermatitis. *Int J Mol Sci* 21(8):2867. <https://doi.org/10.3390/ijms21082867>
 6. Oldhafer KJ, Habel V, Horling K, Makridis G, Wagner KC (2020) Benign liver tumors. *Visc Med* 36(4):292–303. <https://doi.org/10.1159/000509145>
 7. Coppola G, Magis D, Casillo F, Sebastianelli G, Abagnale C, Cioffi E, Di Lenola D, Di Lorenzo C, Serrao M (2022) Neuro-modulation for chronic daily headache. *Curr Pain Headache Rep* 26(3):267–278. <https://doi.org/10.1007/s11916-022-01025-x>
 8. Lefaucheur JP, Aleman A, Baeken C, Benninger DH, Brunelin J, Di Lazzaro V, Filipović SR, Grefkes C, Hasan A, Hummel FC, Jääskeläinen SK, Langguth B, Leocani L, Londero A, Nardone R, Nguyen JP, Nyffeler T, Oliveira-Maia AJ, Oliviero A, Padberg F, ..., Ziemann U (2020) Evidence-based guidelines on the therapeutic use of repetitive transcranial magnetic stimulation (rTMS): an update (2014–2018). *Clin Neurophysiol: Off J Int Federation of Clinical Neurophysiology* 131(2): 474–528. <https://doi.org/10.1016/j.clinph.2019.11.002>
 9. Konstantinou G, Hui J, Ortiz A, Kaster TS, Downar J, Blumberger DM, Daskalakis ZJ (2022) Repetitive transcranial magnetic stimulation (rTMS) in bipolar disorder: a systematic review. *Bipolar disorders* 24(1):10–26. <https://doi.org/10.1111/bdi.13099>
 10. Richter K, Kellner S, Licht C (2023) rTMS in mental health disorders. *Front Network Physiol* 3:943223. <https://doi.org/10.3389/fnetp.2023.943223>
 11. Antal A, Lubner B, Brem AK, Bikson M, Brunoni AR, Cohen Kadosh R, Dubljević V, Fecteau S, Ferreri F, Flöel A, Hallett M, Hamilton RH, Herrmann CS, Lavidor M, Loo C, Lustenberger C, Machado S, Miniussi C, Moliadze V, Nitsche MA, ..., Paulus W (2022) Non-invasive brain stimulation and neuroenhancement. *Clin Neurophysiol Pract* 7:146–165. <https://doi.org/10.1016/j.cnp.2022.05.002>
 12. Velioglu HA, Dudukcu EZ, Hanoglu L, Guntekin B, Akturk T, Yulug B (2024) rTMS reduces delta and increases theta oscillations in Alzheimer's disease: a visual-evoked and event-related potentials study. *CNS Neurosci Ther* 30(1):e14564. <https://doi.org/10.1111/cns.14564>
 13. Wang X, Mao Z, Ling Z, Yu X (2020) Repetitive transcranial magnetic stimulation for cognitive impairment in Alzheimer's disease: a meta-analysis of randomized controlled trials. *J Neurol* 267(3):791–801. <https://doi.org/10.1007/s00415-019-09644-y>
 14. Zhao J, Li Z, Cong Y, Zhang J, Tan M, Zhang H, Geng N, Li M, Yu W, Shan P (2017) Repetitive transcranial magnetic stimulation improves cognitive function of Alzheimer's disease patients. *Oncotarget* 8(20):33864–33871. <https://doi.org/10.18632/oncotarget.13060>
 15. Lin Y, Jin J, Lv R, Luo Y, Dai W, Li W, Tang Y, Wang Y, Ye X, Lin WJ (2021) Repetitive transcranial magnetic stimulation increases the brain's drainage efficiency in a mouse model of Alzheimer's disease. *Acta Neuropathol Commun* 9(1):102. <https://doi.org/10.1186/s40478-021-01198-3>
 16. Yu TW, Lane HY, Lin CH (2021) Novel therapeutic approaches for Alzheimer's disease: an updated review. *Int J Mol Sci* 22(15):8208. <https://doi.org/10.3390/ijms22158208>
 17. Selinger M, Věchtová P, Tykalová H, Ošlejškova P, Rumlová M, Štěrba J, Grubhoffer L (2022) Integrative RNA profiling of TBEV-infected neurons and astrocytes reveals potential pathogenic effectors. *Comput Struct Biotechnol J* 20:2759–2777. <https://doi.org/10.1016/j.csbj.2022.05.052>
 18. Motiwala Z, Aduri NG, Shaye H, Han GW, Lam JH, Katritch V, Cherezov V, Gati C (2022) Structural basis of GABA reuptake inhibition. *Nature* 606(7915):820–826. <https://doi.org/10.1038/s41586-022-04814-x>
 19. Czapski GA, Strosznajder JB (2021) Glutamate and GABA in microglia-neuron cross-talk in Alzheimer's disease. *Int J Mol Sci* 22(21):11677. <https://doi.org/10.3390/ijms222111677>
 20. Andersen JV, Schousboe A, Verkhratsky A (2022) Astrocyte energy and neurotransmitter metabolism in Alzheimer's disease: integration of the glutamate/GABA-glutamine cycle. *Prog Neurobiol* 217:102331. <https://doi.org/10.1016/j.pneurobio.2022.102331>
 21. Ren S, Breuillaud L, Yao W, Yin T, Norris KA, Zehntner SP, D'Adamio L (2021) TNF- α -mediated reduction in inhibitory neurotransmission precedes sporadic Alzheimer's disease pathology in young Trem2^{R47H} rats. *J Biol Chem* 296:100089. <https://doi.org/10.1074/jbc.RA120.016395>
 22. Feng Y, Wei ZH, Liu C, Li GY, Qiao XZ, Gan YJ, Zhang CC, Deng YC (2022) Genetic variations in GABA metabolism and epilepsy. *Seizure* 101:22–29. <https://doi.org/10.1016/j.seizure.2022.07.007>
 23. Pereira JB, Janelidze S, Ossenkopppe R, Kvartsberg H, Brinkmalm A, Mattsson-Carlsson N, Stomrud E, Smith R, Zetterberg H, Blennow K, Hansson O (2021) Untangling the association of amyloid- β and tau with synaptic and axonal loss in Alzheimer's disease. *Brain: J Neurol* 144(1):310–324. <https://doi.org/10.1093/brain/awaa395>
 24. Oakley H, Cole SL, Logan S, Maus E, Shao P, Craft J, Guillozet-Bongaarts A, Ohno M, Disterhoft J, Van Eldik L, Berry R, Vassar R (2006) Intraneuronal beta-amyloid aggregates, neurodegeneration, and neuron loss in transgenic mice with five familial Alzheimer's disease mutations: potential factors in amyloid plaque formation. *J Neurosci: off J Soc Neurosci* 26(40):10129–10140. <https://doi.org/10.1523/JNEUROSCI.1202-06.2006>
 25. Andersen JV, Skotte NH, Christensen SK, Polli FS, Shabani M, Markussen KH, Haukedal H, Westi EW, Diaz-delCastillo M, Sun RC, Kohlmeier KA, Schousboe A, Gentry MS, Tanila H, Freude KK, Aldana BI, Mann M, Waagepetersen HS (2021) Hippocampal disruptions of synaptic and astrocyte metabolism are primary events of early amyloid pathology in the 5xFAD mouse model of Alzheimer's disease. *Cell Death Dis* 12(11):954. <https://doi.org/10.1038/s41419-021-04237-y>
 26. Li K, Wang X, Jiang Y, Zhang X, Liu Z, Yin T, Yang Z (2021) Early intervention attenuates synaptic plasticity impairment and neuroinflammation in 5xFAD mice. *J Psychiatr Res* 136:204–216. <https://doi.org/10.1016/j.jpsychires.2021.02.007>
 27. Zahra A, Jiang J, Chen Y, Long C, Yang L (2018) Memantine rescues prenatal citalopram exposure-induced striatal and social abnormalities in mice. *Exp Neurol* 307:145–154. <https://doi.org/10.1016/j.expneurol.2018.06.003>
 28. Lee JH, Zhang JY, Wei ZZ, Yu SP (2018) Impaired social behaviors and minimized oxytocin signaling of the adult mice deficient in the N-methyl-D-aspartate receptor GluN3A subunit. *Exp Neurol* 305:1–12. <https://doi.org/10.1016/j.expneurol.2018.02.015>
 29. Sun XY, Li LJ, Dong QX, Zhu J, Huang YR, Hou SJ, Yu XL, Liu RT (2021) Rutin prevents tau pathology and neuroinflammation in a mouse model of Alzheimer's disease. *J Neuroinflammation* 18(1):131. <https://doi.org/10.1186/s12974-021-02182-3>
 30. Wei JP, Wen W, Dai Y, Qin LX, Wen YQ, Duan DD, Xu SJ (2021) Drinking water temperature affects cognitive function and progression of Alzheimer's disease in a mouse model. *Acta Pharmacol Sin* 42(1):45–54. <https://doi.org/10.1038/s41401-020-0407-5>

31. Ergin S, Kherad N, Alagoz M (2022) RNA sequencing and its applications in cancer and rare diseases. *Mol Biol Rep* 49(3):2325–2333. <https://doi.org/10.1007/s11033-021-06963-0>
32. Deng YJ, Ren EH, Yuan WH, Zhang GZ, Wu ZL, Xie QQ (2020) GRB10 and E2F3 as diagnostic markers of osteoarthritis and their correlation with immune infiltration. *Diagnostics* (Basel, Switzerland) 10(3):171. <https://doi.org/10.3390/diagnostics10030171>
33. Peng XY, Wang Y, Hu H, Zhang XJ, Li Q (2019) Identification of the molecular subgroups in coronary artery disease by gene expression profiles. *J Cell Physiol* 234(9):16540–16548. <https://doi.org/10.1002/jcp.28324>
34. Zhu M, Ye M, Wang J, Ye L, Jin M (2020) Construction of potential miRNA-mRNA regulatory network in COPD plasma by bioinformatics analysis. *Int J Chron Obstruct Pulmon Dis* 15:2135–2145. <https://doi.org/10.2147/COPD.S255262>
35. Li J, Zhao P, Tian Y, Li K, Zhang L, Guan Q, Mei X, Qin Y (2021) The anti-inflammatory effect of a combination of five compounds from five Chinese herbal medicines used in the treatment of COPD. *Front Pharmacol* 12:709702. <https://doi.org/10.3389/fphar.2021.709702>
36. Tucker S, Möller C, Tegerstedt K, Lord A, Laudon H, Sjö Dahl J, Söderberg L, Spens E, Sahlin C, Waara ER, Satlin A, Gellerfors P, Osswald G, Lannfelt L (2015) The murine version of BAN2401 (mAb158) selectively reduces amyloid- β protofibrils in brain and cerebrospinal fluid of tg-ArcSwe mice. *J Alzheimers Dis: JAD* 43(2):575–588. <https://doi.org/10.3233/JAD-140741>
37. Zhang Y, Ning C, Zhou H, Yan Y, Liu F, Huang Y (2021) Interleukin-1 β , interleukin-6, and interleukin-17A as indicators reflecting clinical response to celecoxib in ankylosing spondylitis patients. *Ir J Med Sci* 190(2):631–638. <https://doi.org/10.1007/s11845-020-02366-5>
38. Huang L, Wang J, Liang G, Gao Y, Jin SY, Hu J, Yang X, Lao J, Chen J, Luo ZC, Fan C, Xiong L, Zhu X, Gao TM, Zhong M, Yang X (2021) Upregulated NMDAR-mediated GABAergic transmission underlies autistic-like deficits in Htr3a knockout mice. *Theranostics* 11(19):9296–9310. <https://doi.org/10.7150/thno.60531>
39. Luo ZY, Huang L, Lin S, Yin YN, Jie W, Hu NY, Hu YY, Guan YF, Liu JH, You QL, Chen YH, Luo ZC, Zhang SR, Li XW, Yang JM, Tao YM, Mei L, Gao TM (2020) Erbin in amygdala parvalbumin-positive neurons modulates anxiety-like behaviors. *Biol Psychiatry* 87(10):926–936. <https://doi.org/10.1016/j.biopsych.2019.10.021>
40. Jo S, Yarishkin O, Hwang YJ, Chun YE, Park M, Woo DH, Bae JY, Kim T, Lee J, Chun H, Park HJ, Lee DY, Hong J, Kim HY, Oh SJ, Park SJ, Lee H, Yoon BE, Kim Y, Jeong Y, ..., Lee CJ (2014) GABA from reactive astrocytes impairs memory in mouse models of Alzheimer's disease. *Nat Med* 20(8):886–896. <https://doi.org/10.1038/nm.3639>
41. Chen ML, Hong CG, Yue T, Li HM, Duan R, Hu WB, Cao J, Wang ZX, Chen CY, Hu XK, Wu B, Liu HM, Tan YJ, Liu JH, Luo ZW, Zhang Y, Rao SS, Luo MJ, Yin H, Wang YY, ..., Liu ZZ (2021) Inhibition of miR-331-3p and miR-9-5p ameliorates Alzheimer's disease by enhancing autophagy. *Theranostics*, 11(5):2395–2409. <https://doi.org/10.7150/thno.47408>
42. Wang Y, Wu Z, Bai YT, Wu GY, Chen G (2017) Gad67 haploinsufficiency reduces amyloid pathology and rescues olfactory memory deficits in a mouse model of Alzheimer's disease. *Mol Neurodegener* 12(1):73. <https://doi.org/10.1186/s13024-017-0213-9>
43. Zou S, Wang C, Cui Z, Guo P, Meng Q, Shi X, Gao Y, Yang G, Han Z (2016) β -Elemene induces apoptosis of human rheumatoid arthritis fibroblast-like synoviocytes *via* reactive oxygen species-dependent activation of p38 mitogen-activated protein kinase. *Pharmacol Rep: PR* 68(1):7–11. <https://doi.org/10.1016/j.pharep.2015.06.004>
44. Liang N, Li Y, Chung HY (2017) Two natural eudesman-type sesquiterpenes from *Laggera alata* inhibit angiogenesis and suppress breast cancer cell migration through VEGF- and Angiopoietin 2-mediated signaling pathways. *Int J Oncol* 51(1):213–222. <https://doi.org/10.3892/ijo.2017.4004>
45. Zhang QF, Li J, Jiang K, Wang R, Ge JL, Yang H, Liu SJ, Jia LT, Wang L, Chen BL (2020) CDK4/6 inhibition promotes immune infiltration in ovarian cancer and synergizes with PD-1 blockade in a B cell-dependent manner. *Theranostics* 10(23):10619–10633. <https://doi.org/10.7150/thno.44871>
46. Huang X, Hernandez CC, Hu N, Macdonald RL (2014) Three epilepsy-associated GABRG2 missense mutations at the γ +/ β - interface disrupt GABAA receptor assembly and trafficking by similar mechanisms but to different extents. *Neurobiol Dis* 68:167–179. <https://doi.org/10.1016/j.nbd.2014.04.015>
47. Ferreira-Vieira TH, Guimaraes IM, Silva FR, Ribeiro FM (2016) Alzheimer's disease: targeting the cholinergic system. *Curr Neuropharmacol* 14(1):101–115. <https://doi.org/10.2174/1570159x13666150716165726>
48. Zhang CQ, McMahon B, Dong H, Warner T, Shen W, Gallagher M, Macdonald RL, Kang JQ (2019) Molecular basis for and chemogenetic modulation of comorbidities in GABRG2-deficient epilepsies. *Epilepsia* 60(6):1137–1149. <https://doi.org/10.1111/epi.15160>
49. Sears SM, Hewett SJ (2021) Influence of glutamate and GABA transport on brain excitatory/inhibitory balance. *Exp Biol Med* (Maywood, N.J.) 246(9):1069–1083. <https://doi.org/10.1177/1535370221989263>
50. Guo B, Zhang M, Hao W, Wang Y, Zhang T, Liu C (2023) Neuroinflammation mechanisms of neuromodulation therapies for anxiety and depression. *Transl Psychiatry* 13(1):5. <https://doi.org/10.1038/s41398-022-02297-y>
51. Jiménez-Balado J, Eich TS (2021) GABAergic dysfunction, neural network hyperactivity and memory impairments in human aging and Alzheimer's disease. *Semin Cell Dev Biol* 116:146–159. <https://doi.org/10.1016/j.semcdb.2021.01.005>
52. Griffiths J, Grant SGN (2023) Synapse pathology in Alzheimer's disease. *Semin Cell Dev Biol* 139:13–23. <https://doi.org/10.1016/j.semcdb.2022.05.028>
53. Südhof TC (2013) Neurotransmitter release: the last millisecond in the life of a synaptic vesicle. *Neuron* 80(3):675–690. <https://doi.org/10.1016/j.neuron.2013.10.022>
54. Lin G, Ji K, Li S, Ma W, Pan X (2020) The genetics analysis of molecular pathogenesis for Alzheimer's disease. *Eur Neurol* 83(5):458–467. <https://doi.org/10.1159/000509799>
55. Knotkova H, Hamani C, Sivanesan E, Le Beuffe MFE, Moon JY, Cohen SP, Huntoon MA (2021) Neuromodulation for chronic pain. *Lancet* (London, England) 397(10289):2111–2124. [https://doi.org/10.1016/S0140-6736\(21\)00794-7](https://doi.org/10.1016/S0140-6736(21)00794-7)
56. Khaleghi A, Zarafshan H, Vand SR, Mohammadi MR (2020) Effects of non-invasive neurostimulation on autism spectrum disorder: a systematic review. *Clin Psychopharmacol Neurosci: off Scientific J Korean College Neuropsychopharmacol* 18(4):527–552. <https://doi.org/10.9758/cpn.2020.18.4.527>
57. Zhang Z, Lin BS, Wu CG, Hsieh TH, Liou JC, Li YT, Peng CW (2022) Designing and pilot testing a novel transcranial temporal interference stimulation device for neuromodulation. *IEEE Trans Neural Syst Rehabil Eng: Pub IEEE Eng Med Biol Soc* 30:1483–1493. <https://doi.org/10.1109/TNSRE.2022.3179537>
58. Rossi S, Antal A, Bestmann S, Bikson M, Brewer C, Brockmüller J, Carpenter LL, Cincotta M, Chen R, Daskalakis JD, Di Lazzaro V, Fox MD, George MS, Gilbert D, Kimiskidis VK, Koch G, Ilmoniemi RJ, Lefaucheur JP, Leocani L, Lisanby SH, ..., basis of this article began with a Consensus Statement from the IFCN Workshop on “Present, Future of TMS: Safety, Ethical Guidelines”, Siena, October 17–20, 2018, updating through April 2020 (2021). Safety and recommendations for TMS use in healthy subjects and patient populations, with updates on training, ethical and regulatory issues: expert Guidelines. *Clin. Neurophysiol: Off J Int*

- Federation of Clinical Neurophysiol 132(1):269–306. <https://doi.org/10.1016/j.clinph.2020.10.003>
59. Michel-Flutot P, Zholudeva LV, Randelman ML, Deramautd TB, Mansart A, Alvarez JC, Lee KZ, Petitjean M, Bonay M, Lane MA, Vinit S (2021) High frequency repetitive Transcranial Magnetic Stimulation promotes long lasting phrenic motoneuron excitability via GABAergic networks. *Respir Physiol Neurobiol* 292:103704. <https://doi.org/10.1016/j.resp.2021.103704>
 60. Pievani M, Mega A, Quattrini G, Guidali G, Ferrari C, Cattaneo A, D'Aprile I, Mascaro L, Gasparotti R, Corbo D, Brignani D, Bortoletto M (2021) Targeting default mode network dysfunction in persons at risk of Alzheimer's disease with transcranial magnetic stimulation (NEST4AD): rationale and study design. *J Alzheimers Dis: JAD* 83(4):1877–1889. <https://doi.org/10.3233/JAD-210659>
 61. Gu L, Wang Y, Shu H (2022) Association between migraine and cognitive impairment. *J Headache Pain* 23(1):88. <https://doi.org/10.1186/s10194-022-01462-4>
 62. Alten B, Zhou Q, Shin OH, Esquivies L, Lin PY, White KI, Sun R, Chung WK, Monteggia LM, Brunger AT, Kavalali ET (2021) Role of aberrant spontaneous neurotransmission in SNAP25-associated encephalopathies. *Neuron* 109(1):59–72.e5. <https://doi.org/10.1016/j.neuron.2020.10.012>
 63. Delgado-Martínez I, Nehring RB, Sørensen JB (2007) Differential abilities of SNAP-25 homologs to support neuronal function. *J Neurosci: Off J Soc Neurosci* 27(35):9380–9391. <https://doi.org/10.1523/JNEUROSCI.5092-06.2007>
 64. O'Leary TP, Brown RE (2022) Visuo-spatial learning and memory impairments in the 5xFAD mouse model of Alzheimer's disease: effects of age, sex, albinism, and motor impairments. *Genes, brain, and behavior* 21(4):e12794. <https://doi.org/10.1111/gbb.12794>
 65. Li X, Qi G, Yu C, Lian G, Zheng H, Wu S, Yuan TF, Zhou D (2021) Cortical plasticity is correlated with cognitive improvement in Alzheimer's disease patients after rTMS treatment. *Brain Stimul* 14(3):503–510. <https://doi.org/10.1016/j.brs.2021.01.012>
 66. Hu Y, Jia Y, Sun Y, Ding Y, Huang Z, Liu C, Wang Y (2022) Efficacy and safety of simultaneous rTMS-tDCS over bilateral angular gyrus on neuropsychiatric symptoms in patients with moderate Alzheimer's disease: a prospective, randomized, sham-controlled pilot study. *Brain Stimul* 15(6):1530–1537. <https://doi.org/10.1016/j.brs.2022.11.009>

Publisher's Note Springer Nature remains neutral with regard to jurisdictional claims in published maps and institutional affiliations.

Springer Nature or its licensor (e.g. a society or other partner) holds exclusive rights to this article under a publishing agreement with the author(s) or other rightsholder(s); author self-archiving of the accepted manuscript version of this article is solely governed by the terms of such publishing agreement and applicable law.